AD-A032 717 NAVAL ACADEMY ANNAPOLIS MD F/G 20/4
CYCLIC LIQUID JET BEHAVIOR IN PULSATING BUBBLES. (U)
MAY 76 N E KARANGELEN
UNCLASSIFIED USNA-TSPR-79 NL

1 OF 2
AD
A032717

1 OF 2

32717

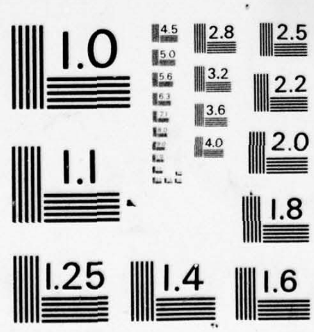

MICROCOPY RESOLUTION TEST CHART
NATIONAL BUREAU OF STANDARDS-1963-A

1 30

A TRIDENT SCHOLAR PROJECT REPORT

NO. 79

"CYCLIC LIQUID JET BEHAVIOR IN PULSATING BUBBLES"

UNITED STATES NAVAL ACADEMY
ANNAPOLIS, MARYLAND
1976

United States. Naval Academy - Trident Scholar project report, no. 79 (1976)

(6) "Cyclic Liquid Jet Behavior in Pulsating Bubbles"

(21) Report on A Trident Scholar Project Report (9) Research rept.

by

Midshipman (10) Nicholas E. Karangelen, Class of 1976

U. S. Naval Academy

Annapolis, Maryland

(14) USNA-TSPR-79

Lawrence A. Crum

Advisor: Assoc. Prof. Lawrence A. Crum
Physics Department

Robert L. Siddon

Advisor: LT R. L. Siddon, Ph.D.
Physics Department

Accepted for Trident Scholar Committee

Chairman

(11) 17 May 76

Date

(12) 99p.

ABSTRACT

This report concerns the behavior of cyclic liquid jets in pulsating bubbles. The jets were developed in bubbles which were situated on a vibrating platform that was contained within a vessel capable of sustaining reduced pressures. The entire assembly was mounted on a variable frequency vibration table and driven at displacement amplitudes on the order of a millimeter. The reduced pressure enabled the jets to be quite easily formed within the vessel; the jets were formed in bubbles containing both vapor and gas, thus resulting in bubbles exhibiting jet behavior over several cycles. The bubbles were photographed with a high speed camera and a detailed analysis made of the behavior of the jet as a function of time. It was found that the bubble surface could be well represented by the first four even terms of a Legendre polynomial expansion. Further, a graphic three-dimensional display of the bubble surface generated by the expansion gives excellent agreement with the observed behavior.

ACKNOWLEDGEMENT

I would like to take this opportunity to thank the following persons for their invaluable assistance during the course of my research:
Richard Krebs, Fred Wasem, Norman Stead, Chuck Stump, Sharon Mark and Steve Satterfield.

However, I would especially like to thank Associate Professor Lawrence A. Crum and Dr. R. L. Siddon for their patience, guidance and moral support and the United States Naval Academy for the financial assistance granted me.

TABLE OF CONTENTS

LIST OF FIGURES

I. HISTORICAL BACKGROUND

A. Interest in Cavitation

The existence of cavitation was first reported by Osborne Reynolds[1] in 1894, who observed small cavities in water flowing in a tube containing a local constriction. The name "cavitation" was given a year later by Froude[2] when, in an investigation of a British destroyer which failed to meet its design speed, Thornycroft and Barnaby[2] postulated that small cavities which formed in the vicinity of the screws limited the thrust. Strange destruction of screws in fast steamboats was described by Silberad[3] in 1912, and in 1919 Cook[4] presented the first attempt at a theoretical approach to cavitation. Lord Raleigh[5] improved and completed this theory for spherical bubble collapse.

Corrections to the Raleigh collapse for surface tension, viscosity and liquid compressibility in gas-filled bubbles have since been made. However, each of these studies has assumed spherical bubble collapse. In actual fact, bubbles often collapse in close proximity to solid boundaries which gives an asymmetrical pressure field and results in non-spherical collapse.

The actual mechanism for cavitation damage has only recently been determined. It was first proposed by Kornfield and Suvarov[6] that a liquid jet formed during bubble collapse was a possible damage mechanism. More recently, Naudé and Ellis[7] studied nonhemispherical cavities collapsing in contact with a solid boundary, and have shown that pressures caused by the cavity wall striking the boundary are higher than those resulting from a compression of gases inside the cavity, and are responsible for the damage.

Recent research efforts have been aimed at developing a model for cavitation bubbles which describes the jet-collapse phenomenon.[8,9,10]

B. Existing Methods of Observation

There are several avenues for measuring cavitation activity.[11] One can record the radiated pressure waves as a cavity collapses or observe the flux of light from the luminescence which may be emitted during the collapse of a transient cavity. The mechanical process of erosion can be noted by measuring the weight loss due to the cavitation effects on a sample. Weissler[12] has measured cavitation events via a chemical reaction in which chlorine is released from carbon tetrachloride dissolved in water.

The best way to observe cavitation events is by visual means. This is no easy task as cavities typically collapse in the order of 50 microseconds. However, cavitation collapse is visually accompanied by an audible "click" and rapidly translating bubbles are easily observed. Attempts at photographing collapsing cavities using ultra-high speed cameras with framing rates of a few million FPS have recently been accomplished. Ellis[13] was able to photograph bubbles in a hydrostatic pressure field and in a gravity force field near a boundary.

This method of photography requires exotic photographic equipment and highly refined timing techniques. The resulting photographs are strongly backlit and the structure of the jet is difficult to discern.

Currently this is the only avenue for direct observation of this phenomenon.

II. INTRODUCTION

Cavitation has been the focus of many research efforts and becomes very significant in the light of the damage which it causes. Cavitation damage costs the U. S. Navy thousands of dollars each year for the replacement of parts eroded by the phenomenon.

Recently it has been determined that the mechanism for the damage is the formation of a jet which impinges on the surface as the bubble collapses. It is appropriate that the focus of the project is on these jets.

Any attempt to investigate further the nature of this jet and its formation must naturally utilize a direct visual observation of the bubble as it collapses. Let us first examine the conditions under which cavitation occurs. Much of damage observed occurs in fluid machinery and is caused by hydrodynamic cavitation. This form of cavitation is due to fluid shear in rapid flow over surfaces. This cavitation phenomenon is very difficult to observe as the bubbles collapse in the rapidly moving liquid.

An alternative to hydrodynamic cavitation is acoustic cavitation, which is induced on rapidly vibrating surfaces. Cavitation bubbles are formed and collapse in a relatively confined space on the face of the vibrating boundary. Thus, acoustic cavitation is the logical choice in attempts to observe cavity collapse.

Cavitation bubble collapse under normal conditions is a very rapid and violent phenomenon. However, the formation of cavities in a fluid can be encouraged by increasing the vapor pressure of the liquid or decreasing the ambient pressure. Thus, under these conditions,

cavitation can be induced at a lower level of acoustic pressure.[14] With this fact in mind, the experimental apparatus described in the following section was designed and built for the purpose of creating cyclic cavities with only a small acoustic pressure, which could be observed with relative ease.

It is the purpose of this paper to first photograph these bubbles and second, to develop a clear, detailed description of cavity collapse.

III. APPARATUS

The feasibility of generating acoustic cavitation at a reduced ambient pressure for the purpose of observing jet behavior in collapsing cavities was demonstrated with a hastily constructed experimental setup hereafter referred to as the original configuration. After careful consideration, a new experimental arrangement was selected, assembled and tested. It was this system which was used to generate the majority of cavities photographed during the course of this project. Ultimately the original configuration of equipment was modified to improve its characteristics and was also used to generate some of the cavities photographed.

A. Original Configuration of Equipment

The original configuration of the equipment is shown in figure 1 . Acoustic pressure is generated inside the containment vessel by the means of a paint shaker to which it is secured. The paint shaker operates at 60 Hz and the amplitude of the vibration can be controlled by means of a potentiometer on the front of the unit. The cylinder which holds the host fluid is of aluminum, 14 cm in diameter and is drilled and fitted with access nozzles to provide a means for insertion and removal of the host fluid, and a means for reducing the ambient pressure inside the vessel. A small platform is positioned inside the cylinder in a horizontal position to provide a site for the formation of cavities which would be readily visible.

The amplitude of vibration is measured via a small accelerometer which outputs to a voltmeter. A linear relationship exists between the output voltage of the accelerometer and the amplitude of the vibration of the system. When the output from the accelerometer was displayed on an oscilloscope, the signal appeared to contain some other frequencies aside from the 60 Hz driving frequency of the shaker table. In order to obtain a better idea of exactly how the system was vibrating, the output from the accelerometer was fed to

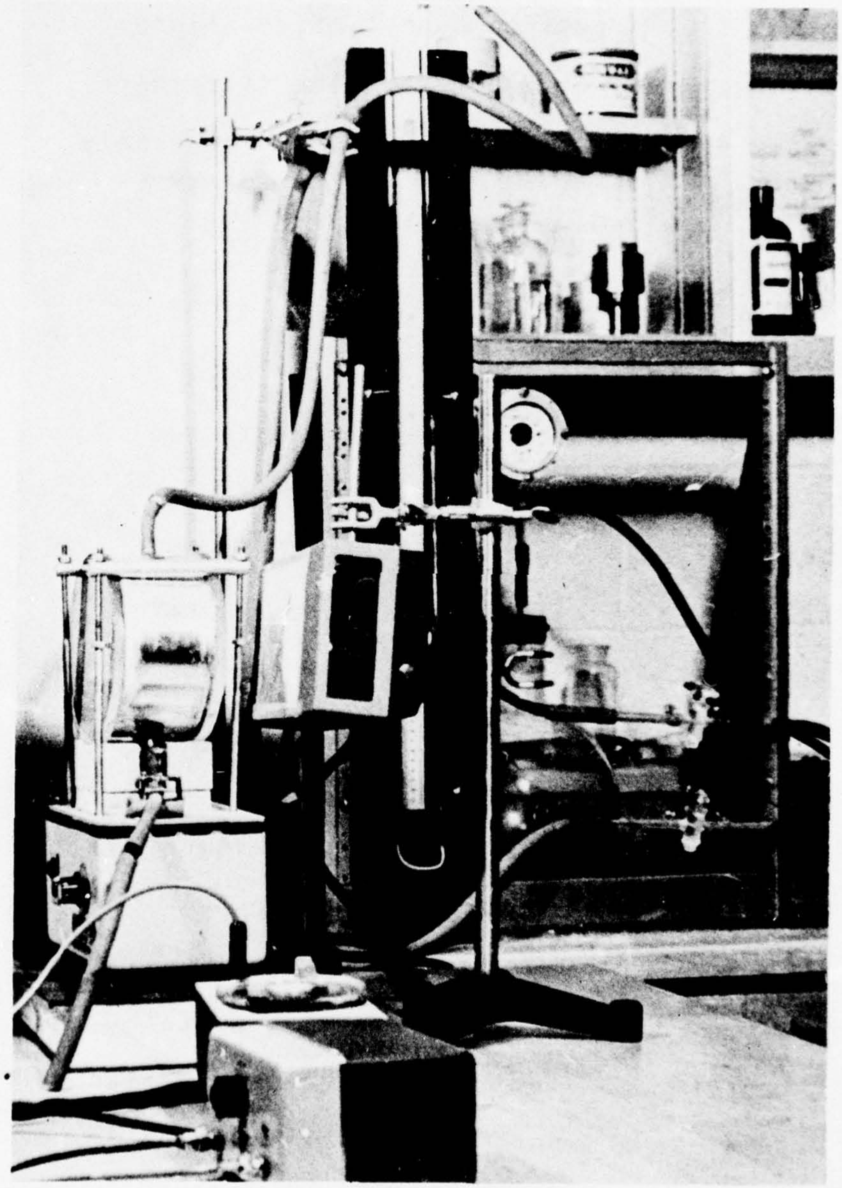

Figure 1. Original configuration of equipment.

a frequency spectrum analyzer and the resultant spectrum displayed via a strip chart recorder. It can be seen from figure 2 that the largest component of the signal is the 60 Hz driving frequency. However, the first harmonic was down only 4 db and the sixth harmonic down only 6 db from the fundamental.

B. System Improvements

In an attempt to improve this spectrum and to add driving frequency flexibility to the system, an M.B. Electronics Vibration Table-Power Amplifier Unit was employed in place of the paint shaker.[15] The existing vessel, when filled with the host fluid, proved to be too massive for the vibration table and could not be driven at a sufficient amplitude to induce acoustic cavitation. A new, lighter design for the containment vessel was needed if the vibration table was to be employed.

The first attempt at a new design for the containment vessel incorporated an aluminum cylinder of smaller radius with plexiglass viewports. This was mounted firmly on an aluminum plate which was secured to the moving element of the vibrating table. Due to this smaller radius, cavities generated in this system were

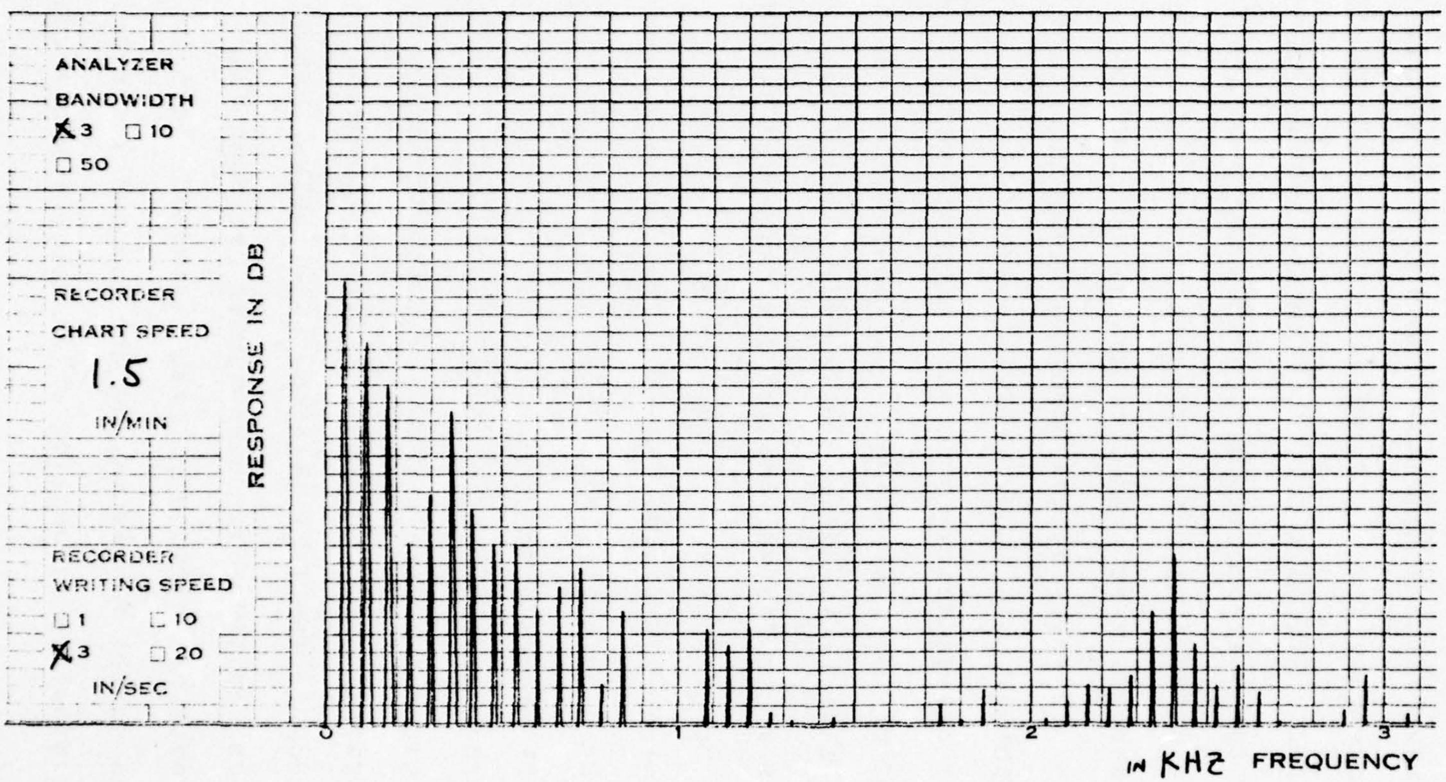

Figure 2. Frequency spectrum analysis of original configuration.

attracted to the walls of the cylinder. They would then migrate away from the center of the platform towards the walls before they grew large enough to be observed and photographed. Attempts to stabilize the bubbles in the center of the platform included giving the platform first a negative, then a positive curvature. However, in each case the bubbles were attracted to the walls of the containment vessel, and thus removed themselves from the area of photographic accessibility.

The final geometry for the containment vessel employed a cylinder of the same diameter as the original vessel (14 mm) but a smaller width. The viewports are of plexiglass as in the smaller vessels mentioned earlier. When this new vessel was clamped firmly to a 1/4 inch thick aluminum plate and secured to the moving element of the vibration table, the system supported the formation of cyclic cavities.

Although this system performed quite well, the cavities generated were not as large as with the original configuration of equipment utilizing the paint shaker. This was due to the fact that the paint shaker provided a vibration amplitude large enough to overcome the buoyant force of relatively large cavities. Thus an avenue was sought for improving the frequency spectrum of the original configuration which could support the

formation of larger cavities.

It was likely that the higher harmonics observed in the frequency spectrum of the original configuration were due to higher modes of oscillation of the system. It was found that these higher modes could be damped considerably by adding additional cross members to the supports which clamped the cylinder to the vibration table. A frequency spectrum analysis of the original configuration, including the additional cross members, is shown in figure 3 . Note that the second harmonic which was so large before is now 9 db down from the fundamental.

Both systems were then available to generate cavities for the high speed photographic study of the jet behavior in a collapsing bubble.

C. Calibration of Shaker Table Amplitude

For each film run, the amplitude of the vibration of the system must be known so that the acoustic pressure inside the cylinder can be determined. This was accomplished by calibrating the output voltage from the accelerometer. Since a linear relationship exists between the output voltage and the vibration amplitude, the amplitude of the vibration was measured at various dial settings and plotted vs the accelerometer output

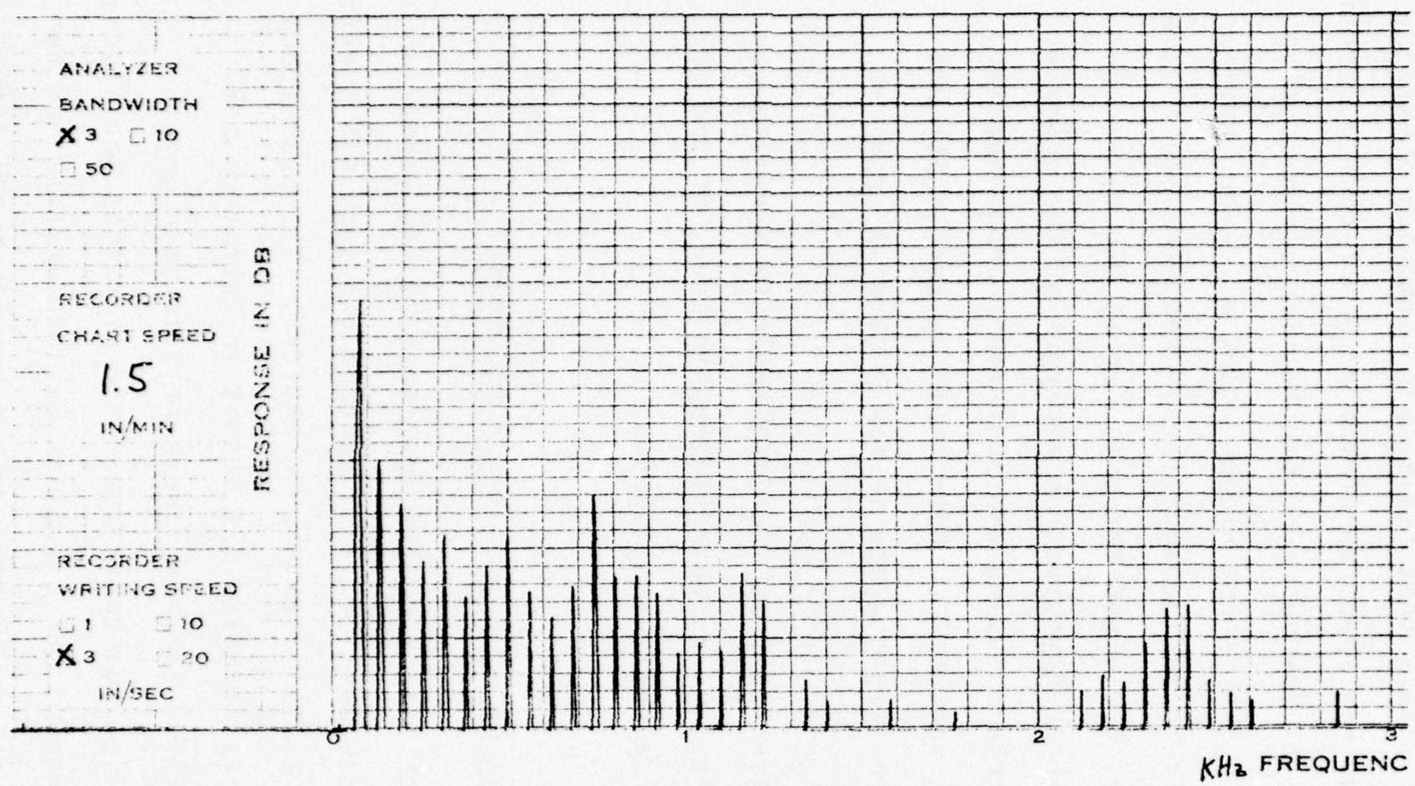

Figure 3. Frequency spectrum of original configuration with additional clamping.

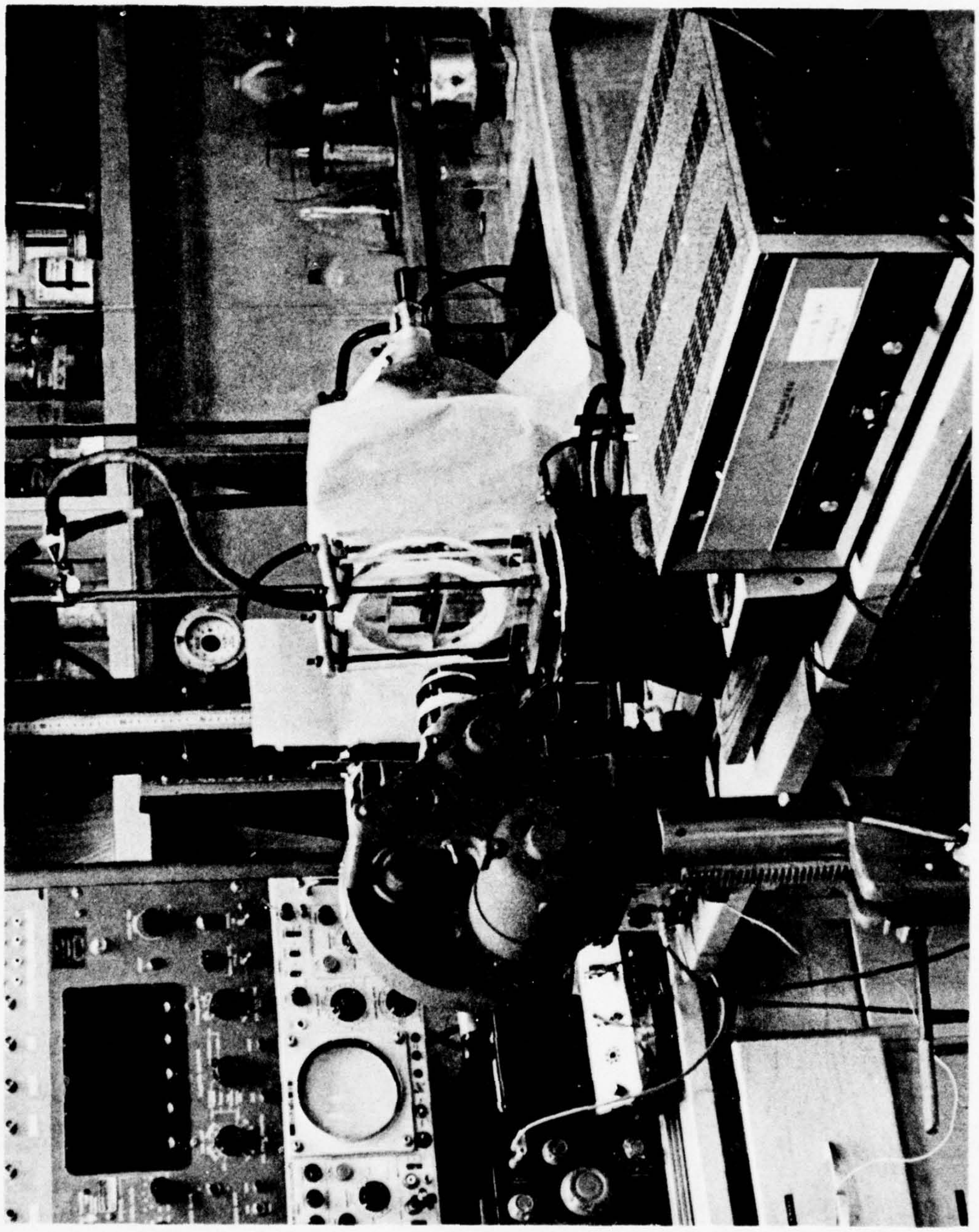

Figure 4. Improved system of equipment.

voltage. A plot of output voltage vs displacement amplitude for the final configuration of equipment appears in figure 5.

IV. THE PHOTOGRAPHIC TECHNIQUE

The cyclic behavior of the bubble lends itself to a photographic technique which utilizes the stroboscopic effect. However, in order to get real time photographs from which data describing the cavity profile in time could be obtained, a high speed camera was employed.

The camera used was a Fastax model W163269 which has a maximum filming capability of about 6000 FPS. An adapter, which also served as an extension tube, was mounted on the camera so that a 50 mm Nikor F/1.4 lens could be utilized. The extension tube-lens system resulted in images on the film which were 52% life size. Additional extension tubes were available. However, their use was prohibited by a lack of sufficient depth of focus.

Due to the magnification of the image on the film by the extension tube, at short ranges, the depth of focus for the camera lens at full aperture was extremely small. This necessitates the use of a large f-number

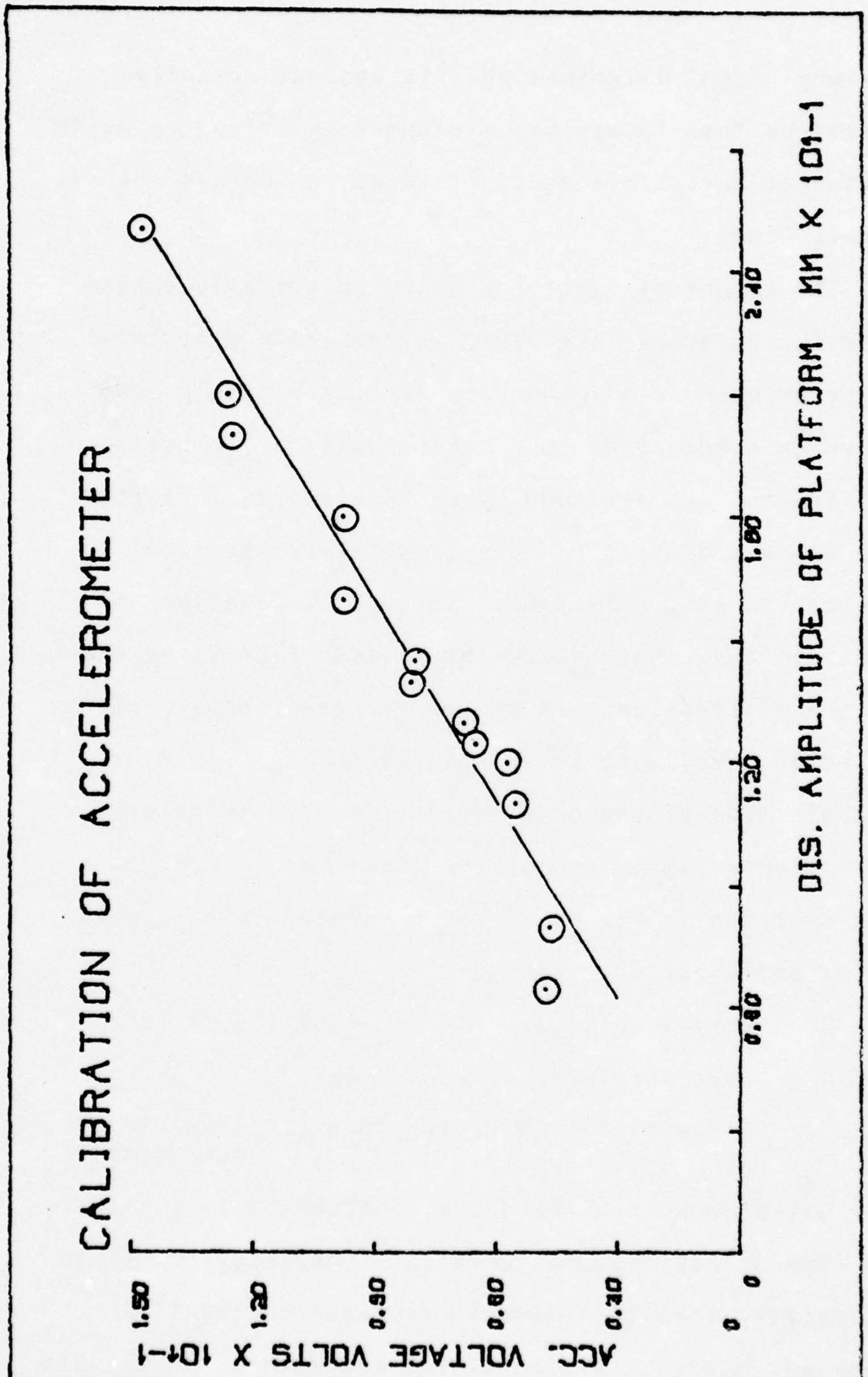
CALIBRATION OF ACCELEROMETER
ACC. VOLTAGE VOLTS X 10↑-1
1.50
1.20
0.90
0.60
0.30
0
0
0.60
1.20
1.80
2.40
DIS. AMPLITUDE OF PLATFORM MM X 10↑-1

Figure 5.

and very bright illumination. It was subsequently determined that f8 was the minimum f-number which would provide an acceptable depth of focus, which was approximately 5 mm.

The amount of light necessary to properly expose Kodak 4-x reversal film #7277 was determined by trial and error, using a filming rate of approximately 5000 FPS which corresponds to a camera voltage of 180V. Illumination was provided by an 8" aluminum reflector with a piece of tracing paper taped over the front to provide for some diffusion. Various combinations of f-numbers and light source intensities (varied by changing the distance between the containment vessel and the reflector face) were tried which resulted in a final determination of the best combination of parameters.

After a comparison of the films resulting from this test, the following set of parameters was arrived at for best results:

Camera Voltage	180V (~5000 FPS)
Lens Aperture	F8
Illumination Distance	10 cm (500W, 8" refractor)

In a situation where the depth of focus is so small, the camera focus becomes critical. An accurate method of insuring that the image is focussed on the film plane was needed. After several attempts to adjust the

camera eye piece failed, a more direct method provided an adequate solution to the problem. A small hole was cut in the film and covered with translucent tape. This served as a "ground glass" on which the image could be focussed directly on the film plane.

V. EXPERIMENTAL OBSERVATIONS AND RESULTS

A. High Speed Photography

Once the equipment and the camera were ready, the actual filming of the cyclic cavities was begun.[16] Nearly 2300 feet of 16 mm film was exposed, developed and studied. Consequently, many different types of behavior were observed in the collapsing cavities.

However, two of the specific types observed seemed to be most prevalent and will be treated here. In the first case, a simple collapse sequence with jet formation is observed toward the final stages of collapse. The second case involves the formation of an inverted jet subsequent to the formation of the impinging jet.

Sequences from actual films appear in figures 6 and 7.

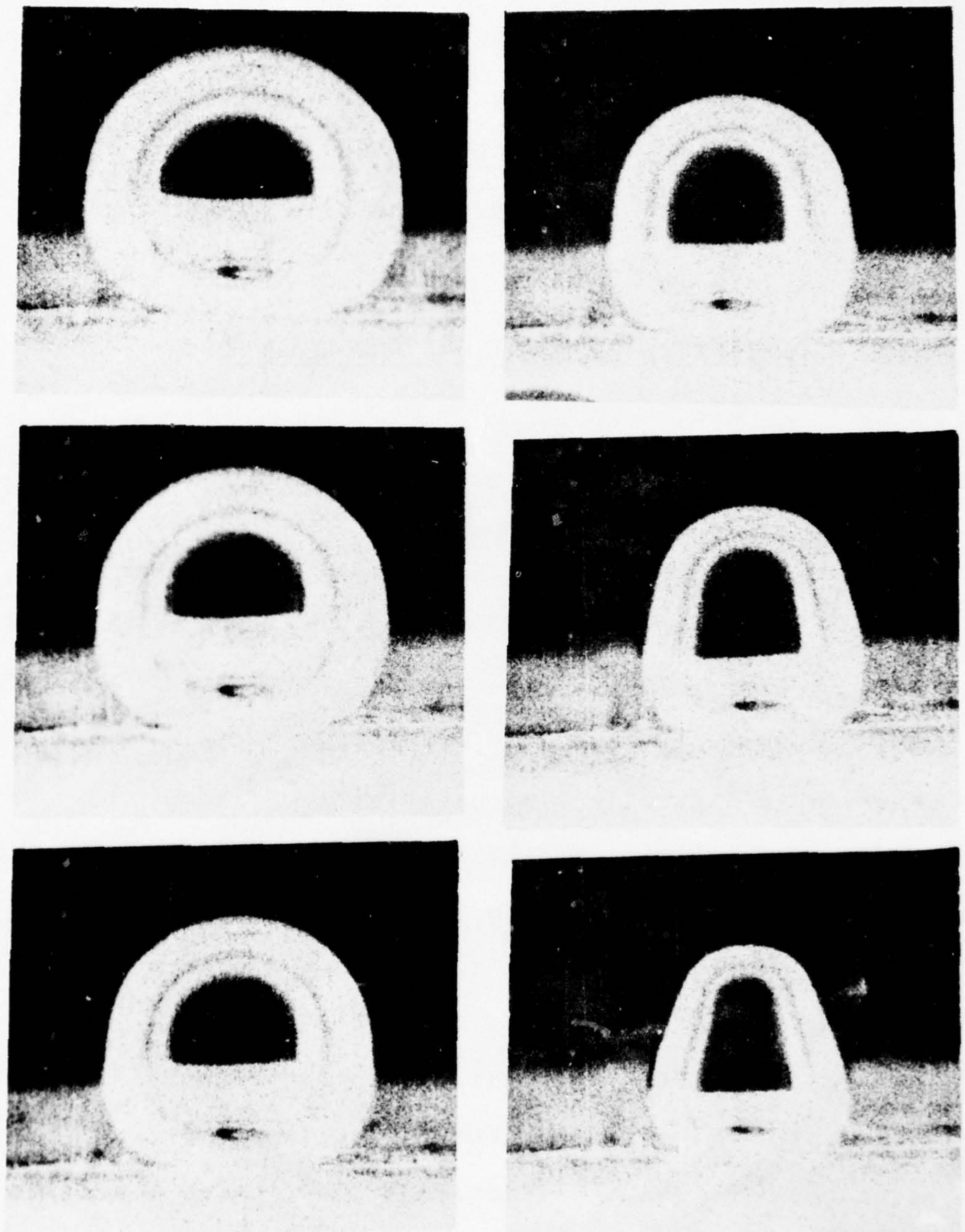

Figure 6. Sequence from Fastax movie film. Time between frames, 265 μS.

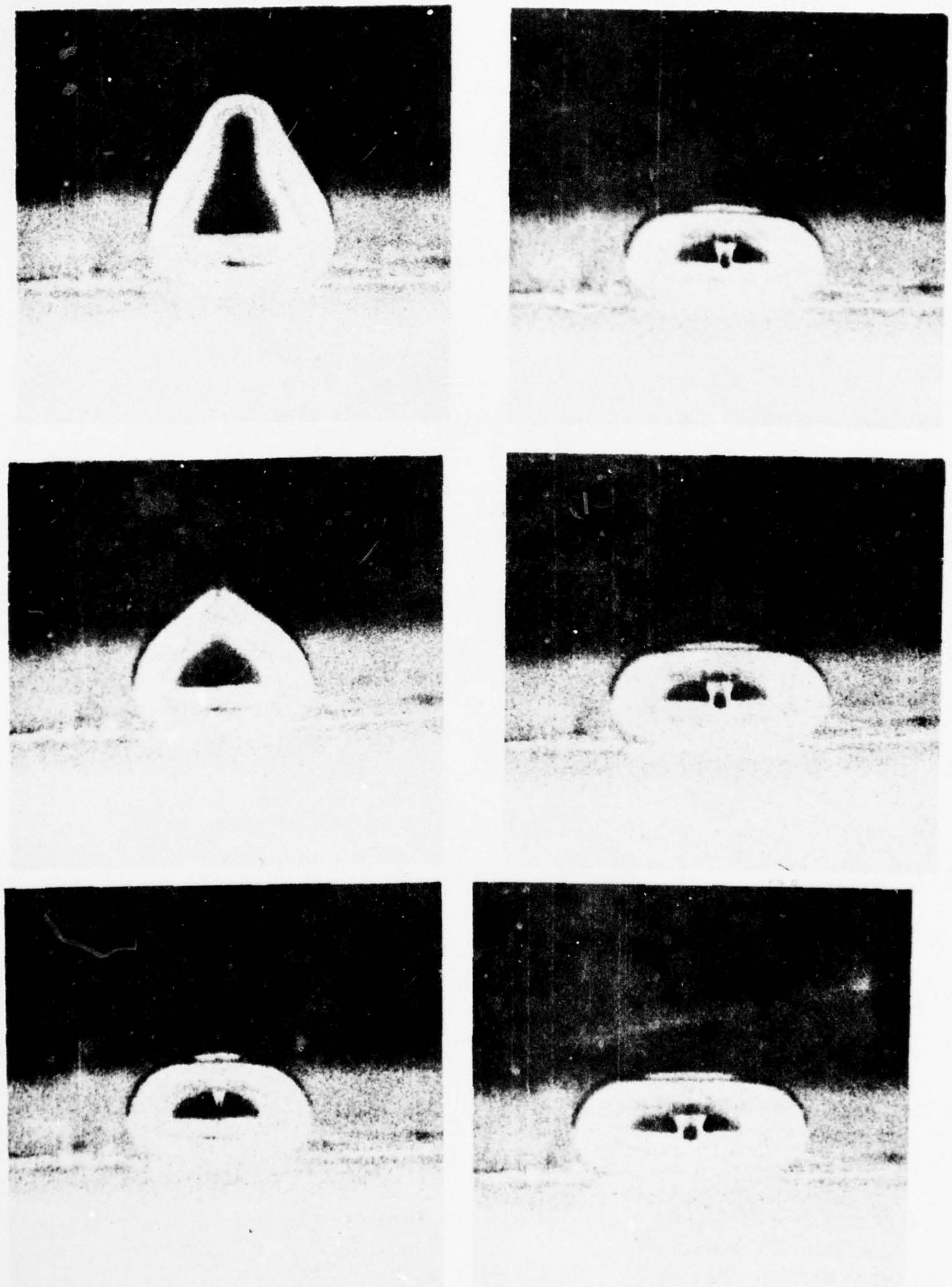

Figure 7. Sequence from Fastax movie film (cont.).

B. Interpretation of Photographs

Once the high speed photographs were taken and a section of film was selected for analysis, a method for digitizing the bubble profile was developed.

First the movie film was enlarged and printed frame by frame to the maximum size possible with a D2V Omega enlarger.

These photographs were then overlayed with a grid, and points on the cavity profile recorded in Cartesian coordinates. It is assumed that due to the wavelength of the driving oscillation, the cavity is essentially in an infinite fluid and has axial symmetry. Based on this assumption, data was taken only from the first quadrant and then reflected across the axis. The height of the cavity in the first photograph of the sequence was then set equal to one, and the rest of the data for that sequence normalized. Since the magnification of the lens is known, the true height of the bubble could be determined from a direct measurement of the film.

Data was taken from sections of film recording the two cases. Case one was without the inverted jet. This data appears in its entirety in Appendix A1, and edited versions in figures 8 and 9.

If the film plane of the camera is not parallel to the vertical axis of the bubble, the actual profile

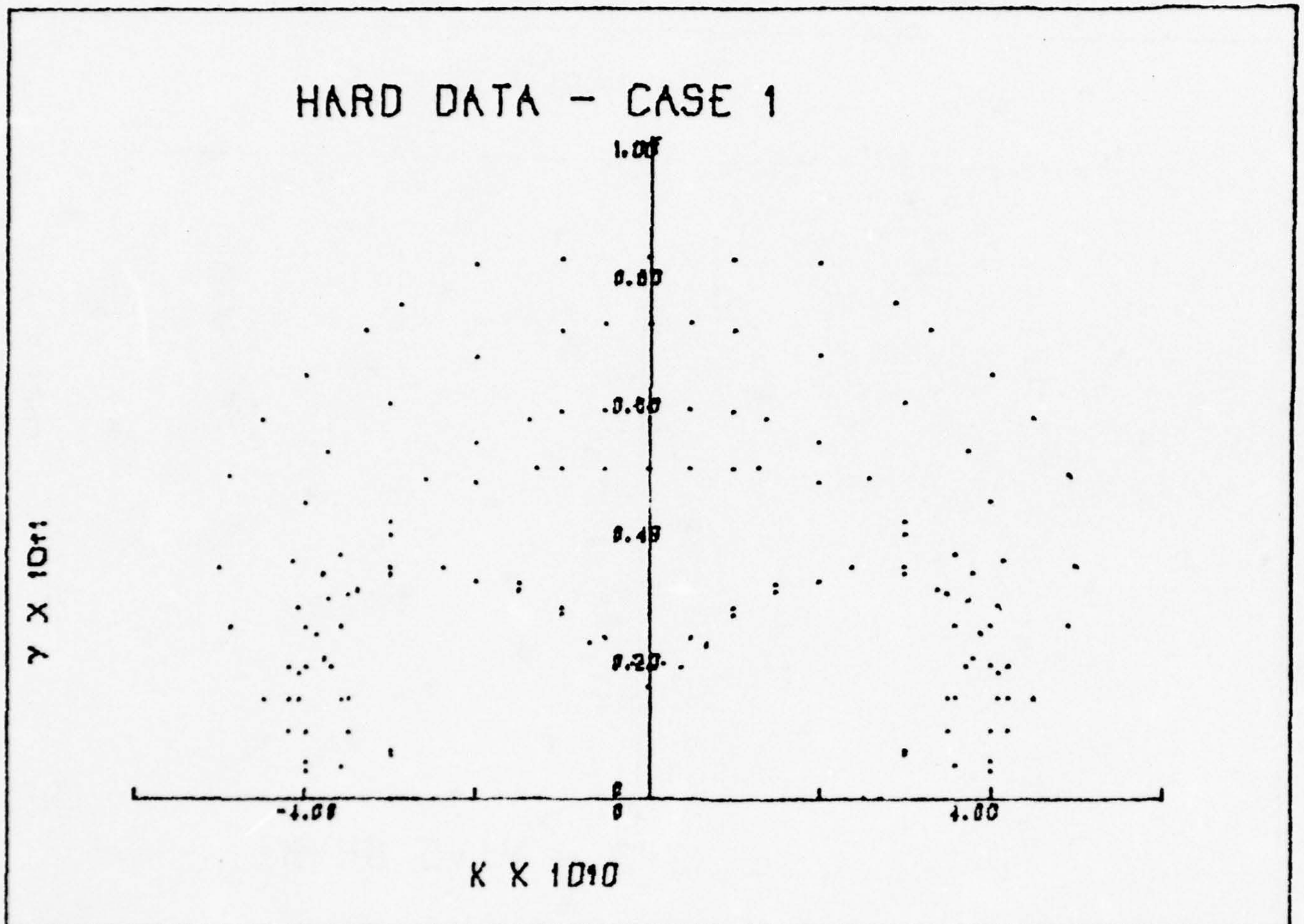

Figure 8. Hard data, case 1, frames 1,3,5,7,9,10.

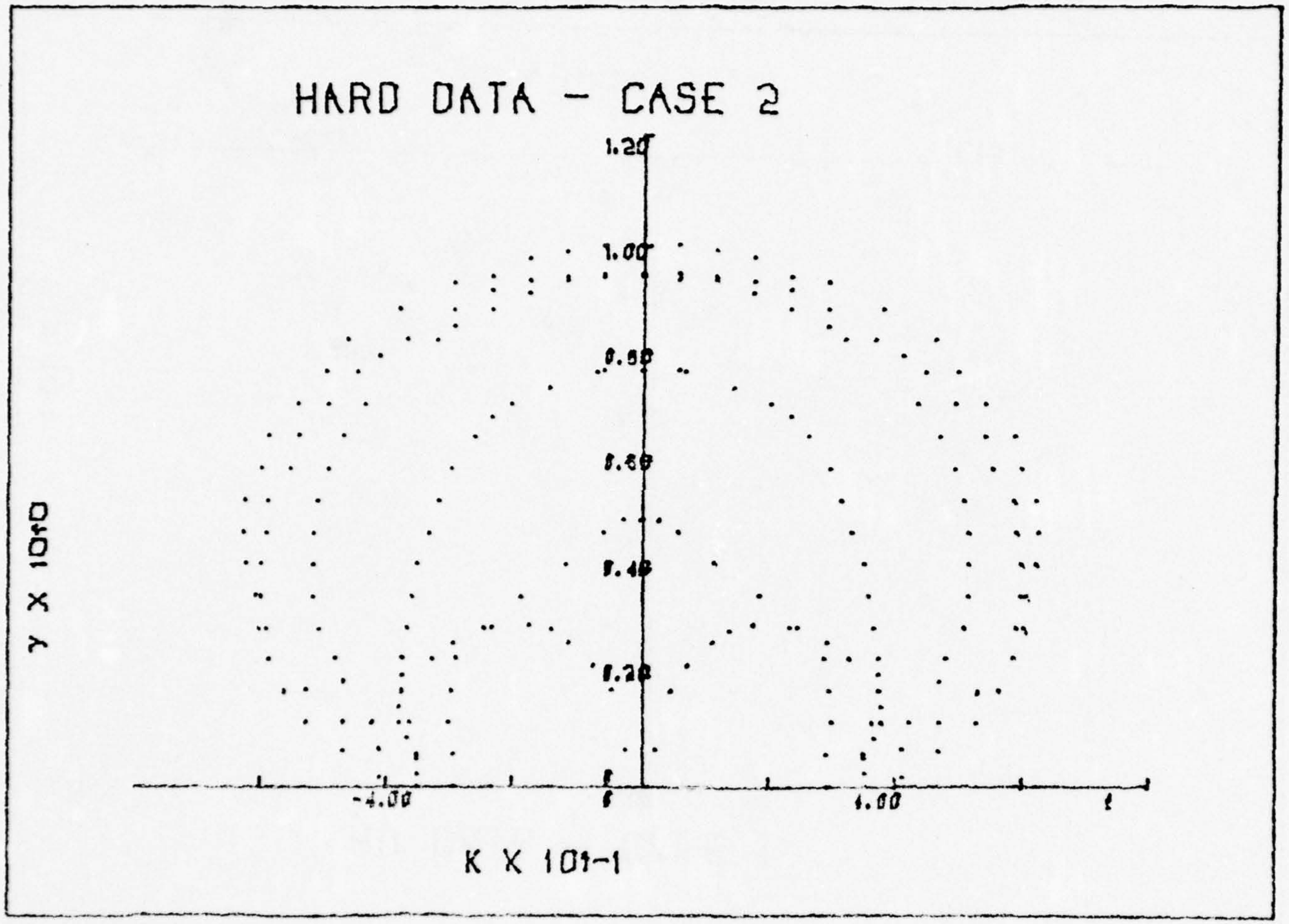

Figure 9. Hard data, case 2, frames 1,3,6,9,12,15.

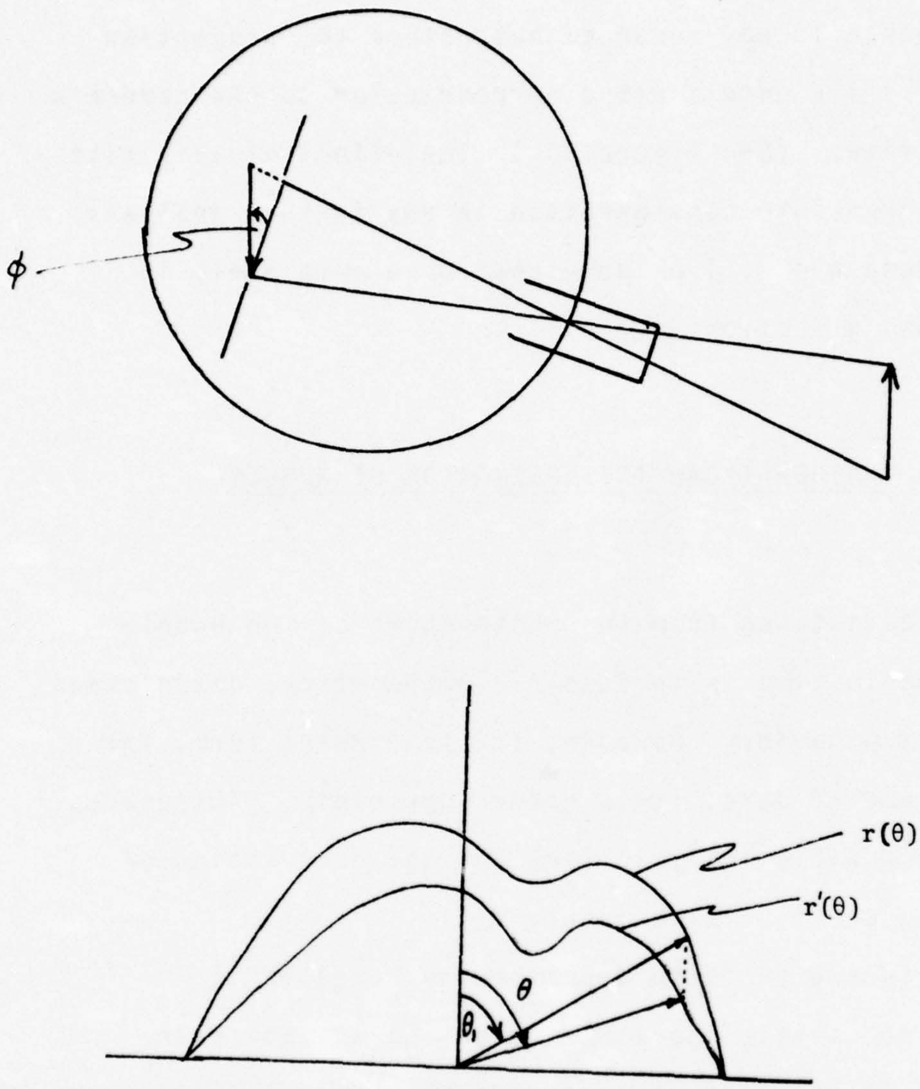

Figure 10. Camera view angle.

of the bubble is not recorded but rather the projection of that profile onto a plane perpendicular to the camera's angle of view. (See figure 10.) The effect of this tilt must be taken into consideration in any further analysis of this data and will be developed more completely in the following section.

VI. MATHEMATICAL INTERPRETATION OF RESULTS

The data taken from the photographs of the bubble collapsing in time is in itself a mathematical description of the jet behavior. However, in its present form, for a large volume of data, it is rather unwieldly. Therefore, a more accessible analytic form for the description of the bubble profile is desirable.

Previous efforts to describe the non-spherical collapse of cavities have been made and the approach here will follow that of Naudé and Ellis.[7]

It has been shown by Naudé and Ellis [7] that for a cavity which is symmetric about a line normal to a solid plane boundary and assuming inviscid, incompressible fluid, a constant pressure inside the cavity, and neglecting surface tension, adhesion and the effect of gravity, that the problem reduces to:

$$\nabla^2\Phi(r,\theta,t) = 0 \quad ,$$

where θ is the polar angle measured from the vertical, and Φ is a scalar potential function such that $\nabla\Phi = \vec{q}$, the velocity vector.

Solving this equation with the appropriate boundary conditions, Ellis[7] has shown that

$$\Phi(r,\theta,t) = \frac{\phi_0(t)}{r} + \sum_{n=1}^{\infty} \Theta_{2n}(t)\,\frac{1}{r^{2n+1}}\,P_{2n}(\cos\theta)$$

where $P_{2n}(\cos\theta)$ are the Legendre polynomials and $\phi_{2n}(t)$ are the time dependent coefficients in the expansion.

The approach leads to an expression for the bubble surface of the form

$$R(\theta,t) = \sum_{n=0}^{\infty} a_{2n}(t)P_{2n}(\cos\theta)$$

Thus the problem is reduced to first determine the best set of coefficients which describe each bubble profile and to second, evaluate these coefficients and determine the validity of truncating the infinite series at a finite number of terms.

Before a rigorous analysis of the data can take place, the question raised earlier of the camera view angle must be treated. In the following discussion the effect of a small rotation in camera angle of the coefficients of the first four even Legendre polynomials will

be considered.

Refer once again to figure 10. If the film plane of the camera is tilted at an angle ϕ with respect to the vertical, the actual image on the film will be the projection of the object back onto a plane parallel to the film plane. This leads to a systematic reduction in the height of the image at any point which is now given by $y(\theta) = y(0)\cos\phi$. This gives rise to a change in each of the Legendre coefficients, which are now given by:

$$a_0' = a_0 + \frac{\phi^2}{4} \quad a_0A_{00} + a_2A_{20} + a_4A_{40} + a_6A_{60}$$

$$a_2' = a_2 + \frac{5\phi^2}{4} \quad a_0A_{02} + a_2A_{22} + a_4A_{42} + a_6A_{62}$$

$$a_4' = a_4 + \frac{9\phi^2}{4} \quad a_0A_{04} + a_2A_{24} + a_4A_{44} + a_6A_{64}$$

$$a_6' = a_6 + \frac{13\phi^2}{4} \quad a_0A_{06} + a_2A_{26} + a_4A_{46} + a_6A_{66}$$

For angles less than 10° this represents a very small change in the coefficients. This is described in detail in Appendix A2.

The method of least squares was used in determining the coefficients for the first four even Legendre polynomials in $\cos\theta$, which best fit each of the profiles analyzed.

As developed earlier the bubble surface can be described by:

$$R(\theta,t) = \sum_{n=0}^{\infty} a_{2n}(t)P_{2n}(\cos\theta)$$

The coefficients $a_{2n}(t)$ were determined from the following analysis:

Let $$S(a_0,a_2,a_4,a_6) = \sum_{i=1}^{N} \{f_i(\theta,a_0,a_2,a_4,a_6) - r_i\}^2$$

where N is the number of points which describes the bubble surface. Thus S represents the sum of the squares of the differences between the function f and the actual surface.

In order to fit f to the points which describe the surface, S must be a minimum which implies $\frac{\partial S}{\partial a_j} = 0$.

Where

$$S(a_0,a_2,a_4,a_6) = a_0P_0(\cos\theta) + a_2P_2(\cos\theta) + a_4P_4(\cos\theta) + a_6P_6(\cos\theta) \quad .$$

Therefore

$$\sum_{i=0}^{N} (a_0P_0 + a_2P_2 + a_4P_4 + a_6P_6 - r_i)P_0 = 0$$

$$\sum_{i=0}^{N} (a_0P_0 + a_2P_2 + a_4P_4 + a_6P_6 - r_i)P_2 = 0$$

$$\sum_{i=0}^{N} (a_0P_0 + a_2P_2 + a_4P_4 + a_6P_6 - r_i)P_4 = 0$$

$$\sum_{i=0}^{N} (a_0P_0 + a_2P_2 + a_4P_4 + a_6P_6 - r_i)P_6 = 0$$

This results in four simultaneous equations in the four coefficients

$$a_0\Sigma P_0^2 + a_2\Sigma P_0P_2 + a_4\Sigma P_0P_4 + a_6\Sigma P_0P_6 = \Sigma r_iP_0$$

$$a_0\Sigma P_0P_2 + a_2\Sigma P_2^2 + a_4\Sigma P_2P_4 + a_6\Sigma P_2P_6 = \Sigma r_iP_2$$

$$a_0\Sigma P_0P_4 + a_2\Sigma P_2P_4 + a_4\Sigma P_4^2 + a_6\Sigma P_4P_6 = \Sigma r_iP_4$$

$$a_0\Sigma P_0P_0 + a_2\Sigma P_2P_6 + a_4\Sigma P_4P_6 + a_6\Sigma P_6^2 = \Sigma r_iP_6$$

Representing this set of equations as a matrix equation we have:

$$S = \begin{array}{cccc} \Sigma P_0^2 & \Sigma P_0P_2 & \Sigma P_0P_4 & \Sigma P_0P_6 \\ \Sigma P_0P_2 & \Sigma P_2^2 & \Sigma P_2P_4 & \Sigma P_2P_6 \\ \Sigma P_0P_4 & \Sigma P_2P_4 & \Sigma P_4^2 & \Sigma P_4P_6 \\ \Sigma P_0P_6 & \Sigma P_2P_6 & \Sigma P_4P_6 & \Sigma P_6^2 \end{array} \qquad A = \begin{array}{c} a_0 \\ a_2 \\ a_4 \\ a_6 \end{array}$$

$$C = \begin{array}{c} \Sigma P_0r \\ \Sigma P_2r \\ \Sigma P_4r \\ \Sigma P_6r \end{array}$$

These equations can now be written in matrix notation:

$$S(4x4) \times A(4x1) = C(4x1)$$

Solving for A:

$$A(4x1) = S^{-1}(4x4) \times C(4x1)$$

Where A(4,1) are the coefficients which best fit the polynomials to the data.

These matrix manipulations lend the problem to numerical solution by computer. A program[17] was written to determine the coefficients and then to generate a plot of the surface using those coefficients. The program also computes the χ^2 as a test of the accuracy of the fit.

This fit of the Legendre polynomials is meaningful only for bubble profiles in which the jet has not yet struck the boundary. At that point, the surface is no longer a single valued function in r and θ, and this analysis is no longer valid. However, once the coefficients are determined for the first ten or so steps which describe the collapse up to the frame just before the jet impinges on the surface, a short extrapolation can be applied and the fit extended right up to the time when the jet contacts the surface of the boundary.

Coefficients were determined in this manner for the

two sets of data describing the two cases. Once the coefficients were solved, a cubic spline fit was used to fill in additional coefficients for the times in between frames.[18] These two resulting sets of coefficients appear graphically in figures 11 and 12 where the actual coefficients for each frame analyzed can be found in Appendix 5.

Figures 13 through 15 show examples of the normalized data and the resulting fit. The values for the X^2 Goodness-of-fit Test for both cases are illustrated in figure 16 and appear in tabulated form in Appendix 6.

A sophisticated, three dimensional graphic display system at the Naval Academy provided an excellent opportunity to portray the history of the bubble collapse via the coefficients which were generated earlier. A photograph of the system is shown in figure 17. A program was prepared for the system's PDP-11 minicomputer to compute and display three dimensional data for the bubble surface from each set of four coefficients.[19] As the computer generated the data for each surface in real time, it was displayed in sequence on a cathode ray tube. Thus, the collapse of the bubble was reconstructed visually using the coefficients which had been generated earlier. From this picture screen, a movie was taken which gives both a profile view and a

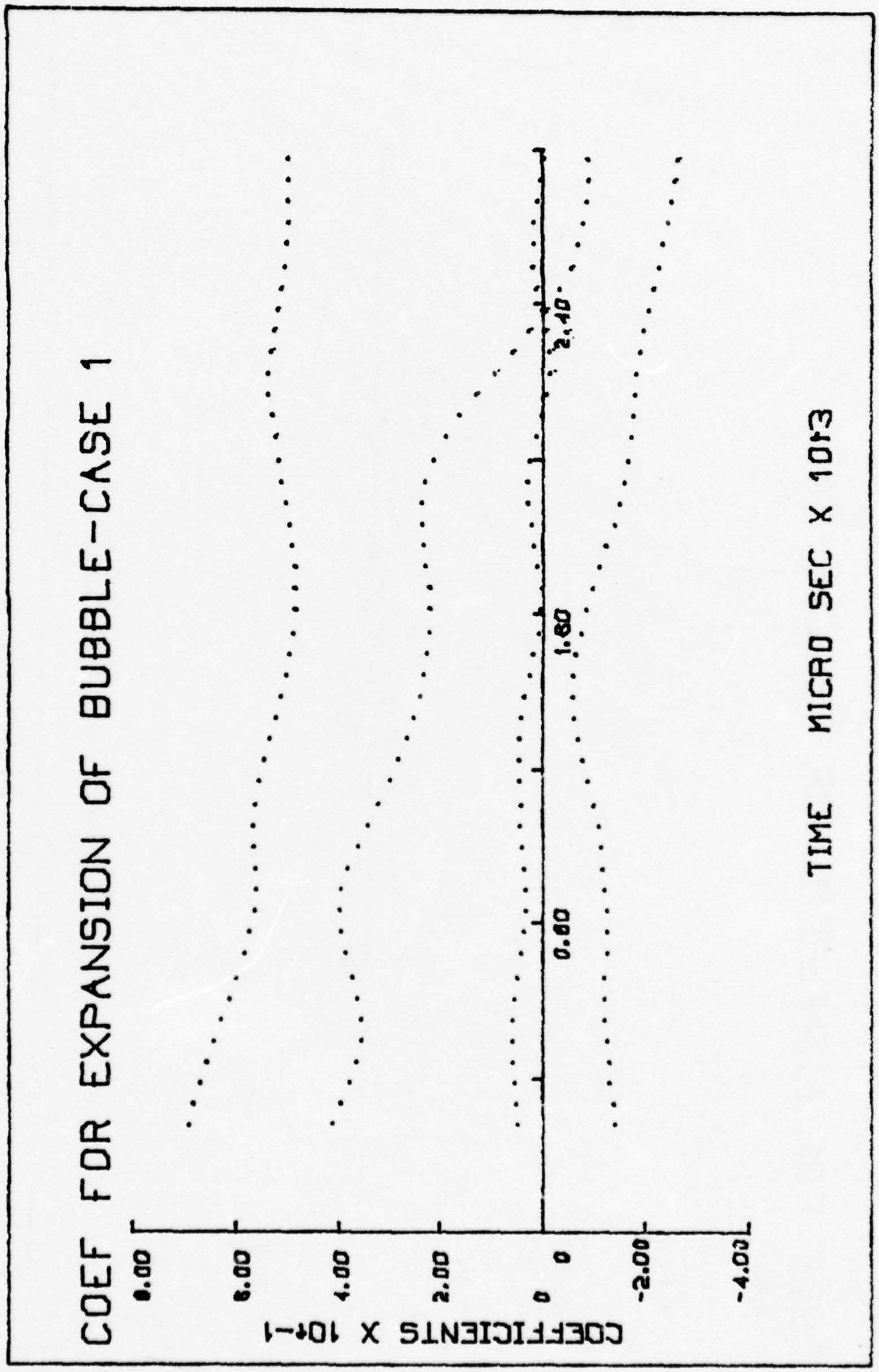
COEF FOR EXPANSION OF BUBBLE-CASE 1
COEFFICIENTS X 10↑-1
8.00
6.00
4.00
2.00
0
-2.00
-4.00
0
0.80
1.60
2.40
TIME MICRO SEC X 10↑3

Figure 11.

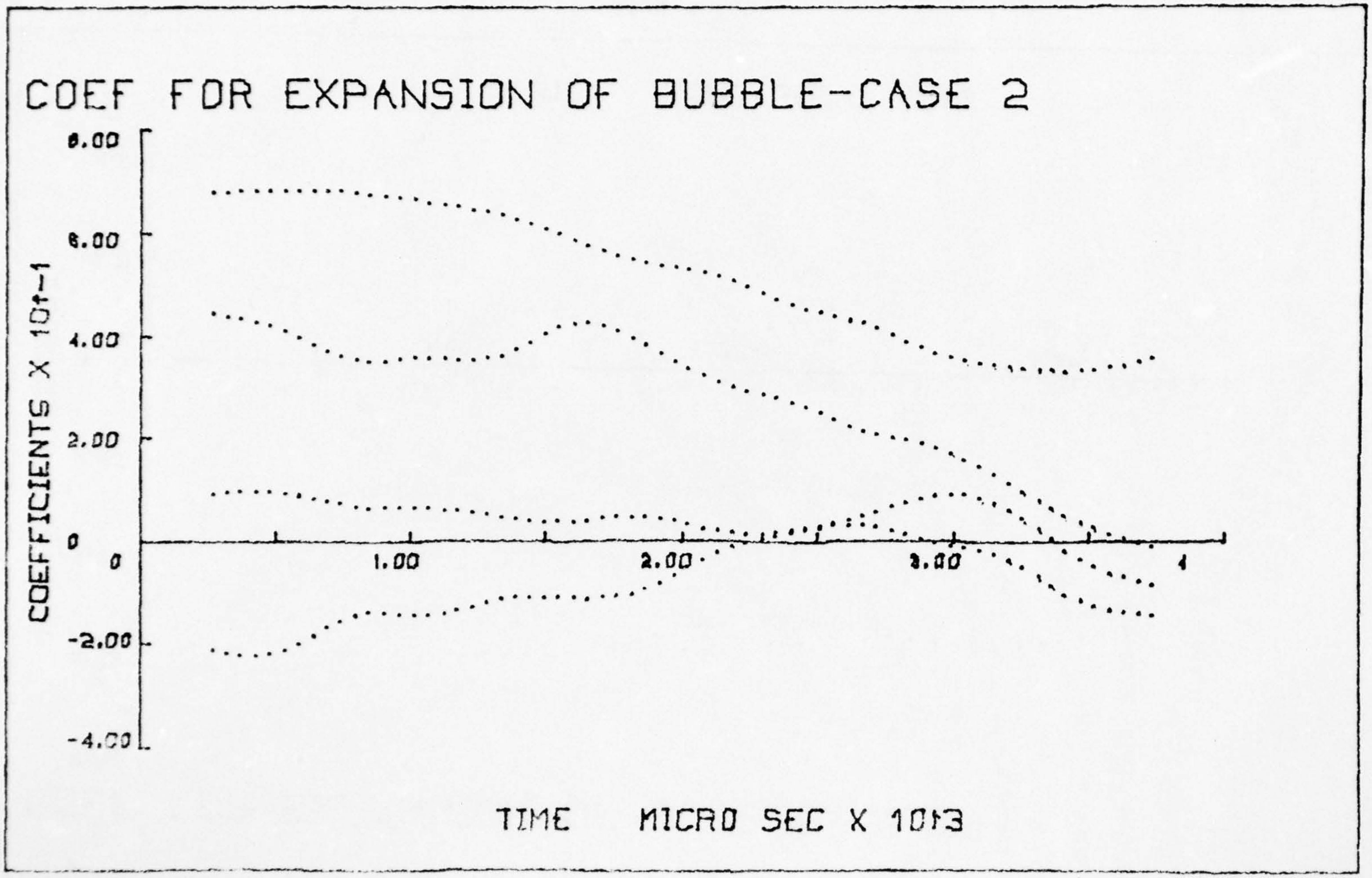
COEF FOR EXPANSION OF BUBBLE-CASE 2
COEFFICIENTS X 10↑-1
8.00
6.00
4.00
2.00
0
-2.00
-4.00
0
1.00
2.00
3.00
4
TIME MICRO SEC X 10↑3

Figure 12.

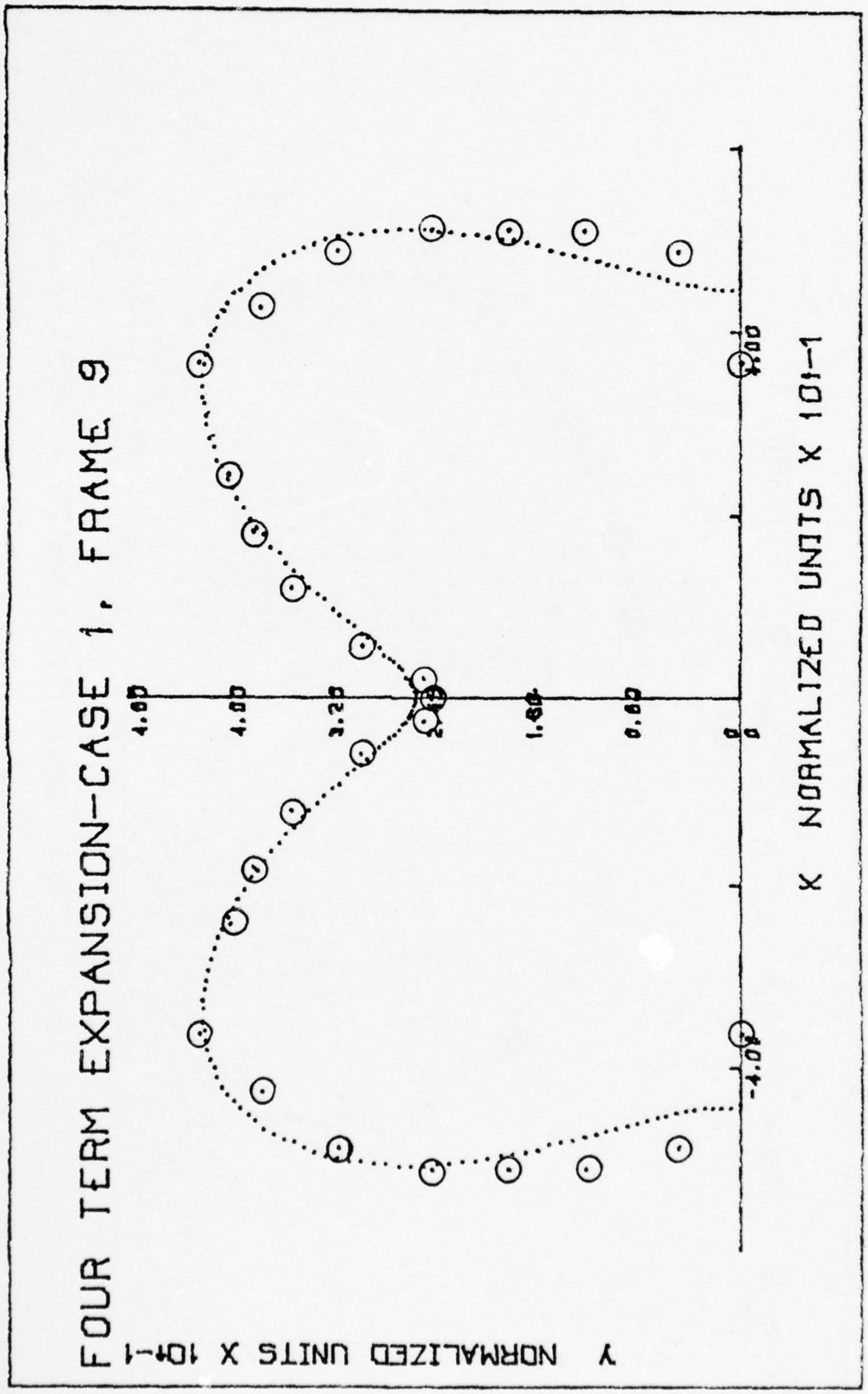
FOUR TERM EXPANSION-CASE 1, FRAME 9
Y NORMALIZED UNITS X 10↑-1
X NORMALIZED UNITS X 10↑-1
4.80
4.00
3.20
2.40
1.60
0.80
0
4.00
-4.00

Figure 13.

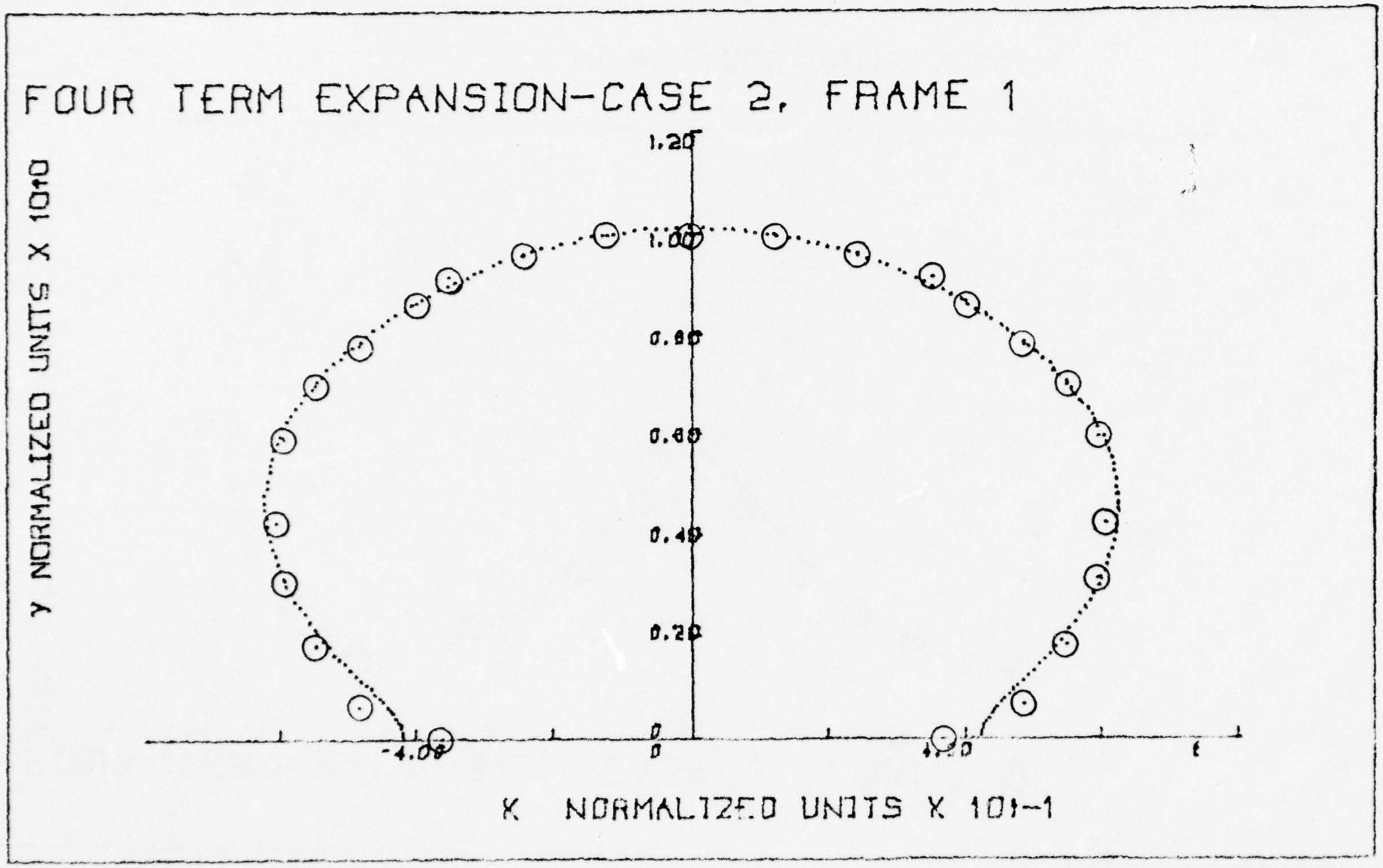
FOUR TERM EXPANSION-CASE 2, FRAME 1
Y NORMALIZED UNITS X 10↑0
1.20
1.00
0.80
0.60
0.40
0.20
0
-4.00
0
4.00
X NORMALIZED UNITS X 10↑-1

Figure 14.

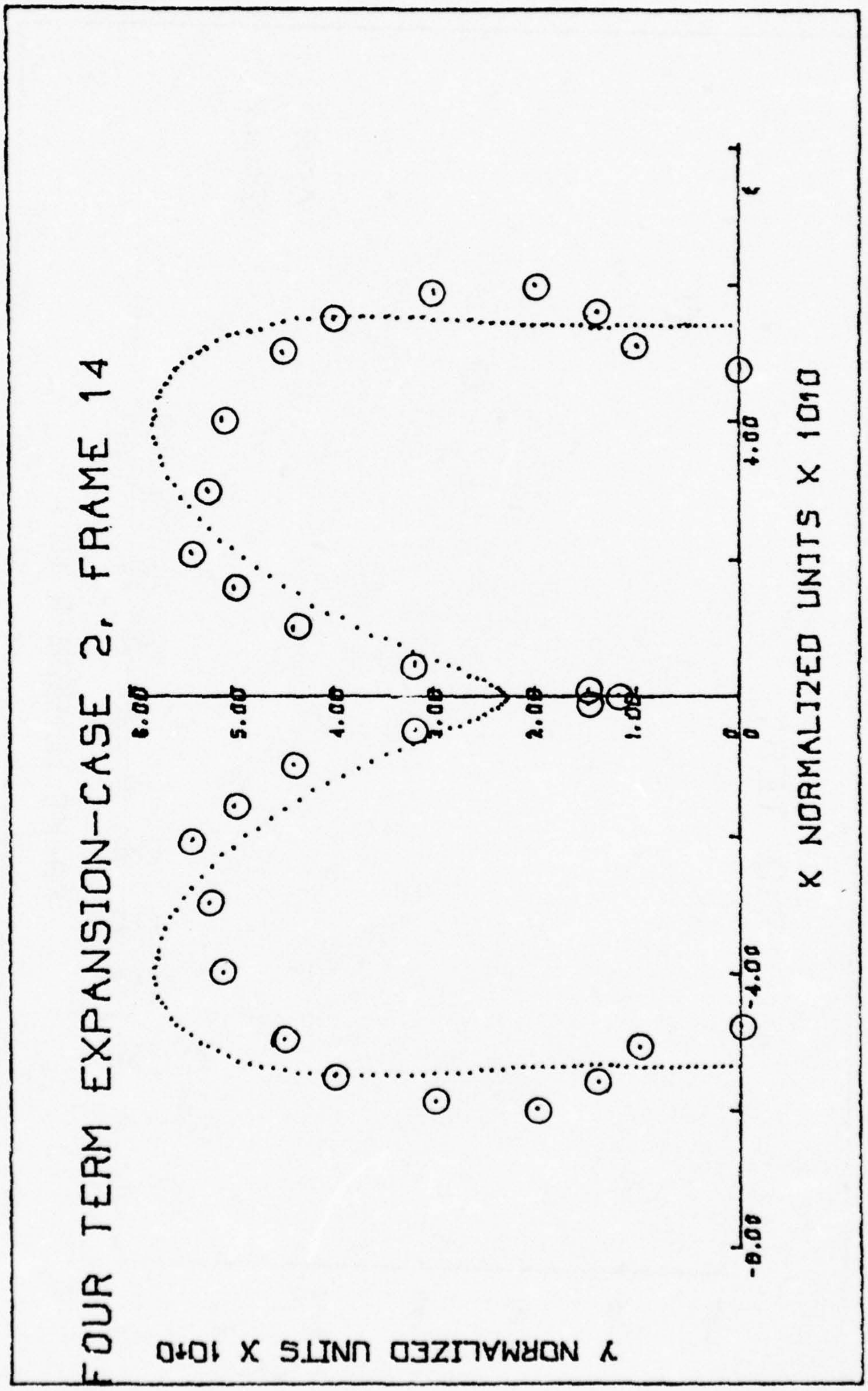
FOUR TERM EXPANSION-CASE 2, FRAME 14
6.00
5.00
4.00
3.00
2.00
1.00
0
-8.00
-4.00
4.00
X NORMALIZED UNITS X 10↑0
Y NORMALIZED UNITS X 10↑0

Figure 15.

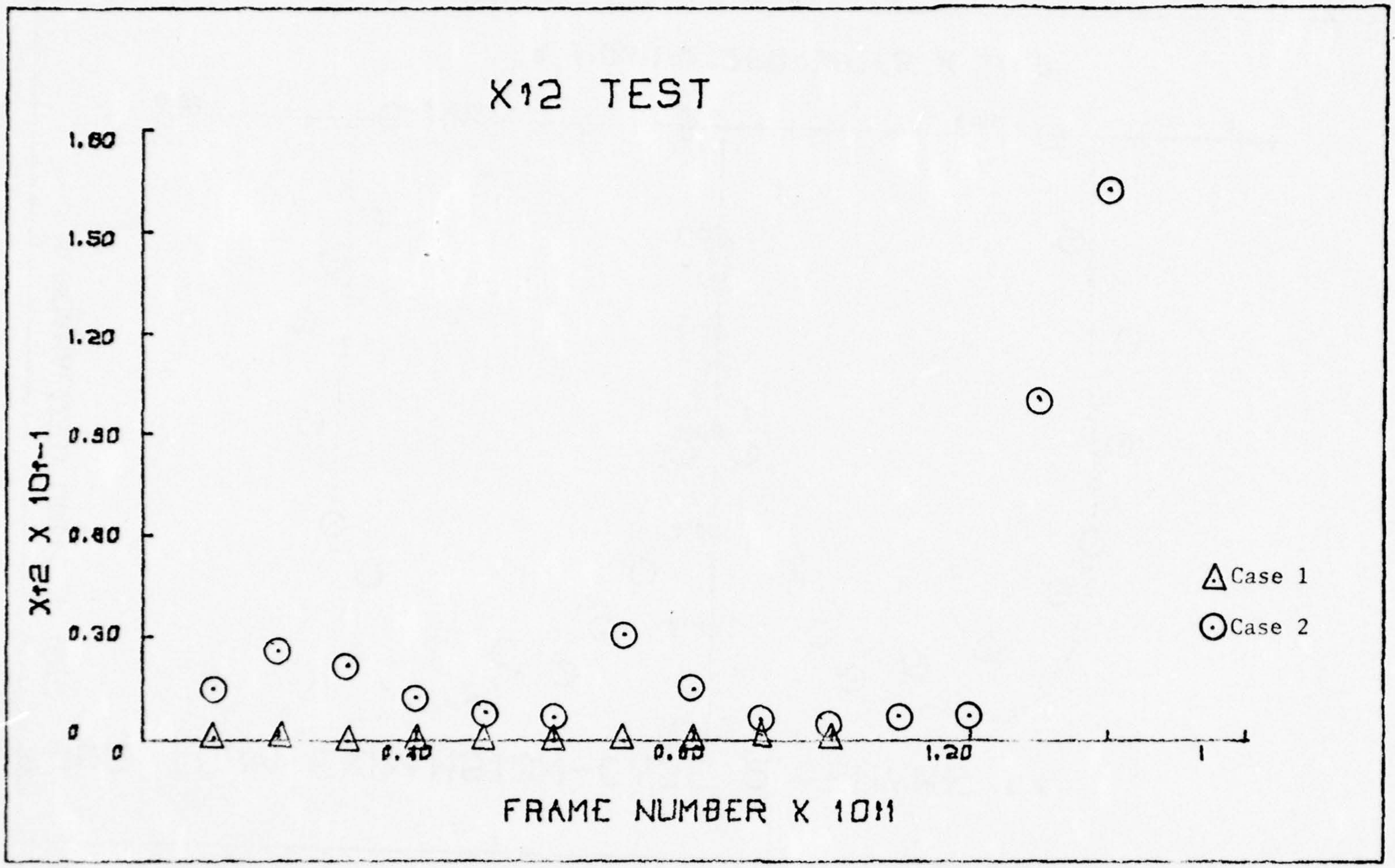

Figure 16. X^2 Goodness-of-fit Test.

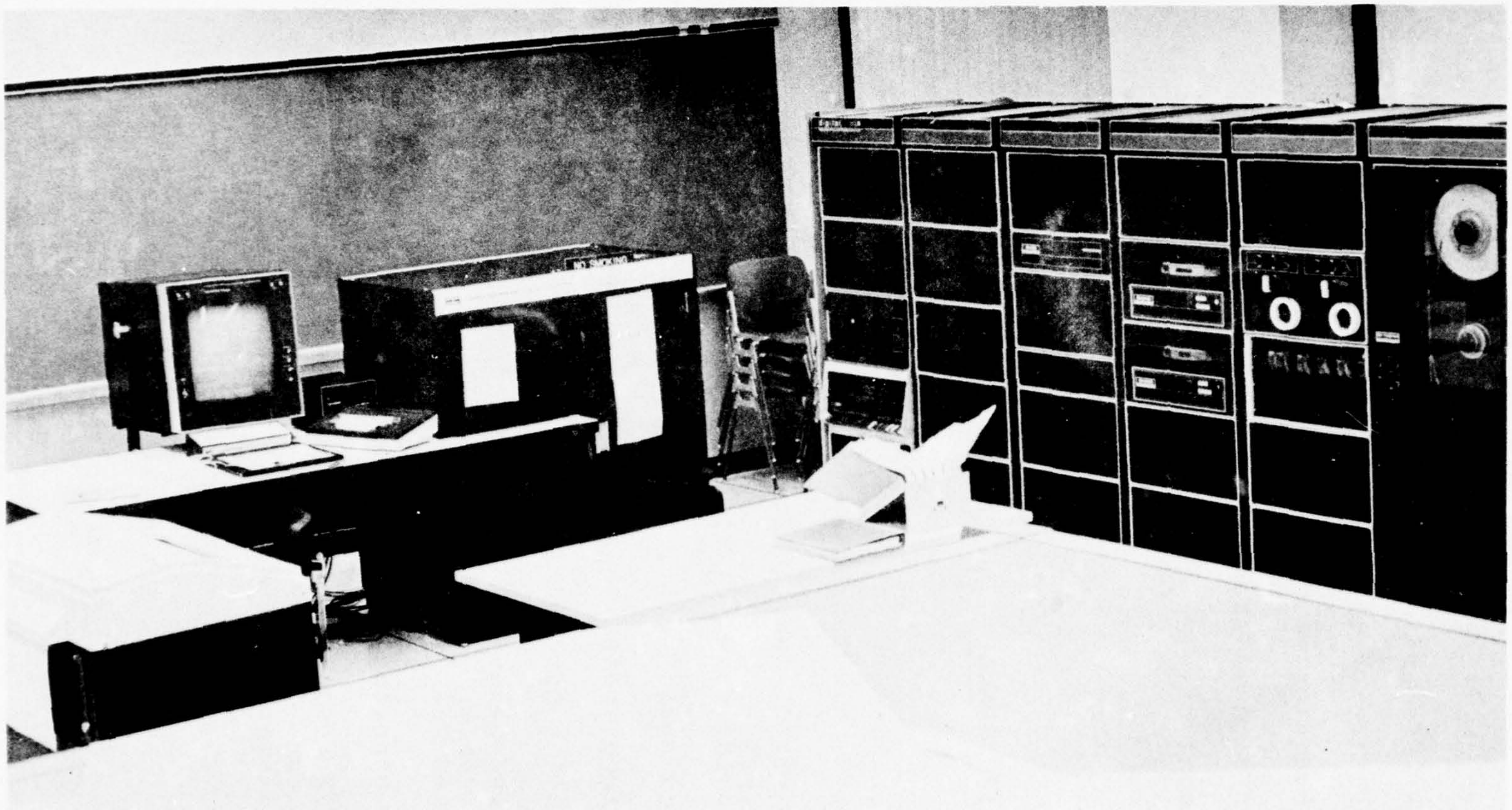

Figure 17. PDP-11/Evans and Sutherland Picture System.

30° look down angle for each collapse case.

A second program was then written to provide for hard copy generation of the 3 dimensional data on a Xynetics flat bed plotter.[20] Selected frames from the collapse sequence could then be reproduced on paper for more permanent display purposes. Examples of these appear in figures 18 and 19.

VII. SUMMARY AND CONCLUSIONS

It is helpful now to review the basic aspects of this project. First, the equipment for the generation of cyclic pulsating cavities at a reduced ambient pressure was designed, built, tested, and modified. Next, it was demonstrated that cyclic cavities could be localized on the horizontal plate inside the containment vessel. The behavior of the oscillating bubbles was then observed and recorded with a Fastax movie camera. After a reliable set of photographic parameters was determined through testing of the camera on the actual system, films were taken for the purpose of obtaining a digitized description of the bubble profile during collapse. Following this, the data was analyzed via a computer program which fit the data to

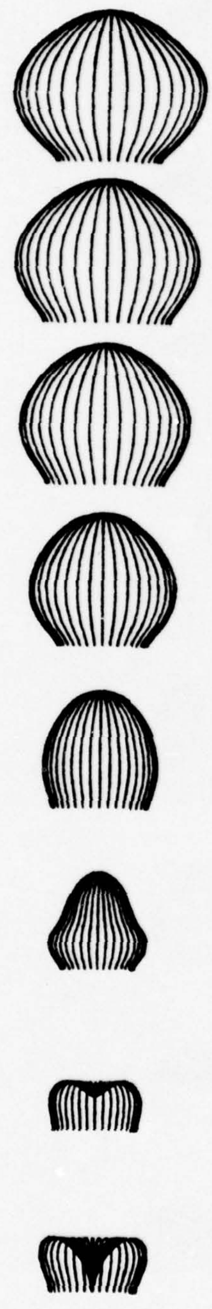

Figure 18. 3 dimensional plots by Xynetics flat bed.

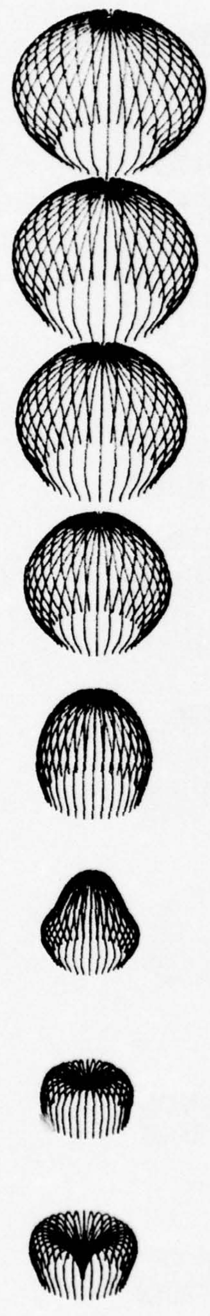

Figure 19. 3 dimensional plots by Xynetics flat bed (cont.).

the first four even Legendre polynomials so that an analytic description of the bubble profile in time could be obtained.

The above outlined method of investigation gave excellent results. As can be seen from the X^2 Goodness-of-fit Test, the fit was remarkably good. Also, by a short extrapolation, the coefficients which describe the complete history of the collapse were obtained. These results are significant in that this type of analysis of raw data has resulted in the generation of Legendre coefficients for the collapse in time. It is at this point that future theoretical approaches to the analytical behavior of collapsing cavities will be compared with theory.

Finally, through the use of the Naval Academy's PDP-11, / E+S Picture System, a 3 dimensional display was generated of the cavity collapse in time as described by the coefficients obtained earlier.

This display provided for a visual comparison between the actual photographs of the collapsing bubble and the resulting fit of the Legendre polynomials.

In conclusion, this graphic representation of cavity collapse, as well as the detailed visual record obtained from the high speed photographs, is unique

with regard to the existing literature and represents a significant advance in cavitation research.

Some preliminary results of this project were reported at the Austin meeting of the Acoustical Society of America and were quite well received. Requests for more details concerning the collapse sequence--the jet behavior has never been seen so clearly before--have been received from a number of researchers. Current plans are to send a copy of edited portions of the filmed jet collapse sequence to these researchers for possible collaboration.

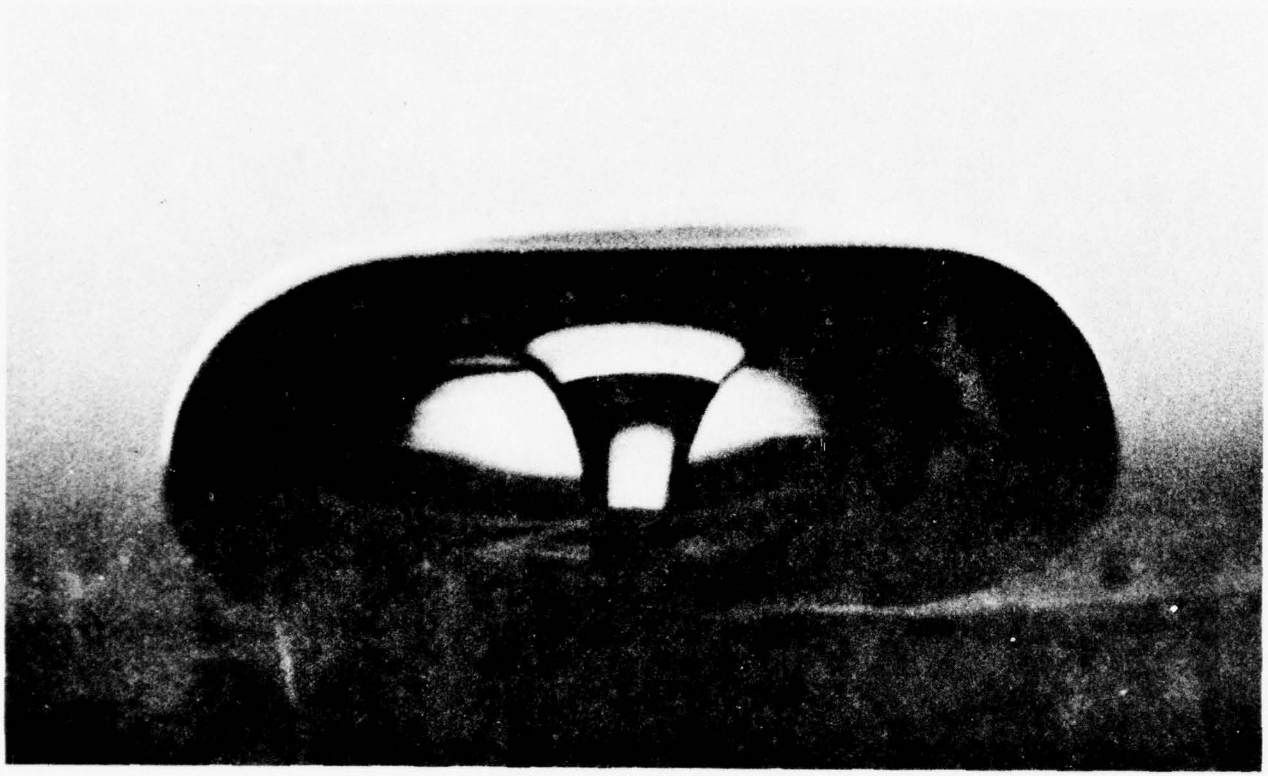

Figure 20. Extreme enlargement of collapsed cavity.

LIST OF REFERENCES

1. O. Reynolds, Sci, Pap., Vol. 2, 587, 1894.

2. Sir John Thornycroft and S. W. Barnaby: "Torpedo Boat Destroyers," *Minutes of Proc. Inst. of Civil Engineers*, Vol. 122, 51-103, 1895.

3. J. Silberad, *Engineering*, 34, 1912.

4. C. A. Parsons and S. S. Cook, "Investigations Into the Causes of Corrosion or Erosion of Propellers," *Trans. Inst. Nav. Arch.*, Vol. 61, 233-240, 1919.

5. Lord Raleigh, "On Pressure Developed In a Liquid During the Collapse of a Spherical Cavity," *Phil. Mag.*, Vol. 34, 94.

6. M. Kornfeld and L. Suvorov, "On the Destructive Action of Cavitation," *J. Appl. Phys.*, 495-503, 1944.

7. C. F. Naudé and A. T. Ellis, "On the Mechanism of Cavitation Damage by Nonhemispherical Cavities Collapsing in Contact With a Solid Boundary," *Trans. ASME*, Vol. 83, Ser. D, *Jr. Basic Engineering*, 648-656, 1961.

8. H. G. Flynn, "Cavitation Dynamics II. Free Pulsations and Models for Cavitation Bubbles," *J. Acoust. Soc. Am.*, Vol. 58, No. 6, Dec. 1975.

9. M. S. Plesset and R. B. Chapman, "Collapse of a Vapor Cavity in the Neighborhood of a Solid Wall," *Calif. Inst. of Tech. Div. of Engr. and Appl. Sci. Rep.*, Vol. 85, 48, Dec. 1969.

10. T. M. Mitchell and F. G. Hammitt, "Collapse of a Spherical Bubble in a Pressure Gradient," *ASME Cavitation Forum*, May 1970.

11. W. P. Manson, *Physical Acoustics Principles and Methods* (New York: Academic Press, 1964), 156-61.

12. A. Weissler, *J. Acoust. Soc. Am.*, Vol. 25, 651 1953.

13. A. T. Ellis, "Parameters Affecting Cavitation and Some Methods for Their Study," *Calif. Inst. of Tech. Hydrogyn. Lab. Rep.,* E-115.1, 1965.

14. Concept originally conceived by Dr. L. A. Crum, United States Naval Academy.

15. The MB Electronics Unit was made available to me by Prof. J. P. Uldrick, United States Naval Academy.

16. The host fluid used in this study was a 5-5-1 mixture of glycerin, water and methanol.

17. Program appears as TRIDENT in Appendix A3.

18. Program was made available to me by Prof. D. F. Rogers and appears as SPLINFIT in Appendix A4.

19. Program appears as AKPLOT in Appendix A7.

20. Program appears as AKFTBD in Appendix A8.

APPENDIX A1

Data taken from enlargements of movie film for both cases considered.

NORMALIZED DATA - CASE 1

FRAME 1

0.365408	0
0.487211	6.69915 E-2
0.548112	0.182704
0.596833	0.316687
0.609013	0.426309
0.596833	0.596833
0.548112	0.700365
0.487211	0.779537
0.401949	0.864799
0.353228	0.91352
0.243605	0.958342
0.121803	0.998782
0	1

*
*

FRAME 2

0.328867	0
0.487211	0.103532
0.535932	0.194884
0.548112	0.304507
0.548112	0.426309
0.535932	0.499391
0.487211	0.621194
0.426309	0.730816
0.365408	0.779537
0.267966	0.852619
0.158343	0.90134
6.09013 E-2	0.91352
0	0.91352

FRAME 3

0.304507	0
0.365403	8.52619 E-2
0.43849	0.182704
0.487211	0.243605
0.499391	0.353228
0.505431	0.43849
0.487211	0.548112
0.45676	0.639464
0.365403	0.730816
0.243605	0.816078
0.121803	0.864799
6.09013 E-2	0.876979
0	0.876979

*

*

FRAME 4

0.328367	0
0.365408	4.87211 E-2
0.43849	0.121803
0.47503	0.219245
0.487211	0.243605
0.493301	0.316687
0.487211	0.365408
0.47503	0.46285
0.426309	0.572473
0.353228	0.688185
0.243605	0.755177
0.146163	0.816078
0.121803	0.813514
6.09013 E-2	0.818514
0	0.813514

FRAME 5

0.334957	0
0.426309	0.121803
0.45067	0.243605
0.43849	0.316687
0.414129	0.383678
0.365408	0.487211
0.316687	0.590743
0.243605	0.657734
0.170524	0.700365
0.121803	0.712546
6.09013 E-2	0.718636
*0	0.72229
*	

FRAME 6

0.328367	0
0.377588	9.74421 E-2
0.414129	0.182704
0.426309	0.292326
0.414129	0.365408
0.365408	0.499391
0.280146	0.560292
0.182704	0.609013
0.121803	0.615104
6.09013 E-2	0.621194
0	0.621194

FRAME 7

0.328867	0
0.365408	7.91717 E-2
0.426309	0.182704
0.46285	0.255786
0.47503	0.304507
0.46285	0.414129
0.43849	0.45067
0.365408	0.511571
0.243605	0.584653
0.158343	0.609013
0.121803	0.609013
6.09013 E-2	0.609013
0	0.609013

*

FRAME 8

0.389769	0
0.45067	7.30816 E-2
0.487211	0.146163
0.505481	0.255786
0.47503	0.353228
0.43849	0.43849
0.365408	0.499391
0.304507	0.535932
0.243605	0.523752
0.182704	0.499391
0.121803	0.47503
6.09013 E-2	0.45067
0	0.43849

FRAME 9

0.365408	0
0.487211	4.87211 E-2
0.511571	0.121803
0.512789	0.182704
0.511571	0.243605
0.487211	0.316687
0.426309	0.377588
0.365408	0.426309
0.243605	0.401949
0.182704	0.383678
0.121803	0.353228
6.09013 E-2	0.298417
2.43605 E-2	0.249695
0	0.243605

*

FRAME 10

0.365408	0
0.43849	6.09013 E-2
0.487211	0.121803
0.499391	0.182704
0.499391	0.231425
0.45676	0.365408
0.365408	0.426309
0.292326	0.426309
0.182704	0.395859
0.121803	0.353228
0.121803	0.353228
8.52619 E-2	0.286236
4.87211 E-2	0.243605
0	0.207065

NORMALIZED DATA - CASE 2

FRAME 1

0.294118	0
0.352941	2.35294 E-2
0.411765	7.05882 E-2
0.470588	0.117647
0.529412	0.176471
0.588235	0.235294
0.605882	0.294118
0.608824	0.352941
0.623529	0.411765
0.629412	0.470588
0.623529	0.529412
0.6	0.588235
0.588235	0.647059
0.541176	0.705882
0.5	0.764706
0.464706	0.823529
0.382353	0.882353
0.294118	0.929412
0.235294	0.941176
0.176471	0.976471
0.117647	0.988235
5.88235 E-2	1
0	1

*

*

FRAME 2

0.294118	0
0.352941	2.35294 E-2
0.411765	5.88235 E-2
0.470588	0.1
0.529412	0.147059
0.583235	0.235294
0.547059	0.176471
0.611765	0.294118
0.623529	0.352941
0.629412	0.411765
0.617647	0.470588
0.611765	0.529412
0.594118	0.594118
0.582353	0.647059
0.529412	0.705882
0.488235	0.764706
0.417647	0.829412
0.352941	0.882353
0.294118	0.911765
0.235294	0.935294
0.176471	0.952941
0.117647	0.958824
5.88235 E-2	0.964706
0	0.964706

FRAME 3

0.352941	0
0.411765	1.76471 E-2
0.470588	6.47059 E-2
0.529412	0.117647
0.564706	0.176471
0.588235	0.235294
0.594118	0.294118
0.6	0.352941
0.6	0.411765
0.594118	0.470588
0.588235	0.529412
0.552941	0.588235
0.541176	0.647059
0.494118	0.705882
0.447059	0.764706
0.370588	0.823529
0.294118	0.882353
0.235294	0.917647
0.176471	0.935294
0.117647	0.941176
5.88235 E-2	0.947059
0	0.947059

*
*

FRAME 4

0.352941	0
0.411765	3.52941 E-2
0.470588	3.82353 E-2
0.529412	0.158824
0.541176	0.176471
0.564706	0.235294
0.576471	0.294118
0.588235	0.352941
0.588235	0.411765
0.570588	0.470588
0.564706	0.529412
0.547059	0.588235
0.523529	0.641176
0.476471	0.711765
0.423529	0.764706
0.352941	0.823529
0.294118	0.864706
0.235294	0.894118
0.176471	0.917647
0.117647	0.929412
5.88235 E-2	0.935294
0	0.935294

FRAME 5

0.352941	0
0.411765	4.11765 E-2
0.470588	0.111765
0.529412	0.211765
0.5	0.152941
0.535294	0.235294
0.547059	0.294118
0.552941	0.352941
0.552941	0.411765
0.547059	0.470588
0.535294	0.529412
0.523529	0.588235
0.5	0.647059
0.452941	0.705882
0.4	0.764706
0.329412	0.823529
0.235294	0.882353
0.176471	0.9
0.117647	0.923529
5.88235 E-2	0.938235
0	0.941176

*

FRAME 6

0.294118	0
0.352941	5.88235 E-2
0.423529	0.117647
0.470588	0.194118
0.482353	0.235294
0.511765	0.294118
0.517647	0.352941
0.517647	0.411765
0.517647	0.470588
0.508824	0.529412
0.470588	0.647059
0.494118	0.588235
0.435294	0.705882
0.411765	0.794118
0.323529	0.823529
0.235294	0.882353
0.176471	0.911765
0.294118	0.852941
0.117647	0.932353
5.88235 E-2	0.941176
0	0.941176

FRAME 7

WHAT?

0.235294	0
0.294118	2.94118 E-2
0.352941	5.88235 E-2
0.411765	8.82353 E-2
0.441176	0.176471
0.464706	0.235294
0.470588	0.294118
0.470588	0.352941
0.470588	0.411765
0.464706	0.470588
0.447059	0.529412
0.408824	0.647059
0.435294	0.588235
0.364706	0.705882
0.305882	0.764706
0.235294	0.823529
0.176471	0.841176
0.117647	0.864706
5.88235 E-2	0.882353
0	0.882353

*

FRAME 8

0.294118	0
0.352941	2.94118 E-2
0.388235	5.88235 E-2
0.411765	0.117647
0.423529	0.176471
0.429412	0.235294
0.429412	0.294118
0.423529	0.352941
0.417647	0.411765
0.411765	0.470588
0.388235	0.529412
0.376471	0.588235
0.347059	0.647059
0.294118	0.705882
0.235294	0.764706
0.176471	0.794118
0.117647	0.817647
5.88235 E-2	0.823529
0	0.823529

FRAME 9

```
 0.294118   0
 0.352941   5.88235 E-2
 0.364706   0.117647
 0.376471   0.176471
 0.379412   0.205882
 0.376471   0.235294
 0.370588   0.294118
 0.361765   0.352941
 0.352941   0.411765
 0.335294   0.470588
 0.320588   0.529412
 0.3       0.588235
 0.264706   0.647059
 0.235294   0.685294
 0.205882   0.705882
*0.147059   0.735294
 7.35294 E-2  0.764706
 5.88235 E-2  0.767647
 0          0.767647
*
```

FRAME 10

```
0.294118   0
0.335294   5.88235 E-2
0.358824   0.117647
0.352941   0.176471
0.35      0.235294
0.329412   0.294118
0.311765   0.352941
0.294118   0.411765
0.267647   0.470588
0.247059   0.529412
0.229412   0.588235
0.191176   0.647059
0.147059   0.685294
9.41176 E-2  0.705882
5.88235 E-2  0.717647
0          0.717647
```

FRAME 11

0.235294	0
0.294118	5.88235 E-2
0.294118	0.247059
0.323529	0.147059
0.320588	0.176471
0.305882	0.235294
0.294118	0.294118
0.258824	0.352941
0.226471	0.411765
0.179412	0.470588
0.147059	0.529412
*0.117647	0.588235
8.82353 E-2	0.629412
5.88235 E-2	0.652941
0	0.652941
*	

FRAME 12

0.235294	0
0.294118	5.88235 E-2
0.302941	0.117647
0.3	0.176471
0.291176	0.235294
0.247059	0.294118
0.191176	0.352941
0.117647	0.411765
5.88235 E-2	0.470588
2.94118 E-2	0.494118
0	0.494118

FRAME 13

0.235294	0
0.294118	0.05
0.323529	3.82353 E-2
0.323529	0.117647
0.305882	0.176471
0.294118	0.205882
0.235294	0.282353
0.176471	0.311765
0.117647	0.314706
7.05882 E-2	0.314706
5.29412 E-2	0.3
2.94118 E-2	0.264706
1.17647 E-2	0.235294
5.88235 E-3	0.188235
0	0.152941

*

FRAME 14

0.282353	0
0.335294	2.94118 E-2
0.352941	7.64706 E-2
0.352941	0.117647
0.347059	0.176471
0.323529	0.235294
0.294118	0.264706
0.235294	0.3
0.176471	0.308824
0.123529	0.317647
9.41176 E-2	0.294118
5.88235 E-2	0.258824
2.94118 E-2	0.188235
5.88235 E-3	8.82353 E-2
0	7.05882 E-2

FRAME 15

0.294118	0
0.352941	5.29412 E-2
0.370588	8.82353 E-2
0.382353	0.117647
0.382353	0.147059
0.376471	0.176471
0.329412	0.235294
0.294118	0.264706
0.235294	0.294118
0.176471	0.3
0.141176	0.288235
0.114706	0.264706
7.64706 E-2	0.223529
4.70588 E-2	0.176471
2.35294 E-2	7.05882 E-2
1.47059 E-2	0

*

APPENDIX A2

Correction for camera view angle.

$$r(\theta_1)\sin\theta_1 = r'(\theta)\sin\theta$$

$$\tan\theta_1 = \tan\theta\cos\phi$$

$$r(\theta_1)\cos\theta_1\cos\phi = r'(\theta)\cos\phi$$

$$r'(\theta) = r(\theta_1)\sqrt{\sin^2\theta_1 + \cos^2\theta_1\cos^2\phi}$$

$$r'(\theta) = r\{\tan^{-1}(\tan\theta\cos\phi)\}\sqrt{\frac{\tan^2\theta\cos^2\phi}{1+\tan^2\theta\cos^2\phi} + \frac{\cos^2\phi}{1+\tan^2\theta\cos^2\phi}}$$

First evaluate

$$\frac{\tan^2\theta\cos^2\phi}{1+\tan^2\theta\cos^2\phi} + \frac{\cos^2\phi}{1+\tan^2\theta\cos^2\phi}$$

$$= \frac{\cos^2\phi\{1+\tan^2\theta\}}{1 + \tan^2\theta\cos^2\phi}$$

$$= \frac{\cos^2\phi}{\cos^2\theta + \sin^2\theta\cos^2\phi}$$

$$= \frac{\cos^2\phi}{\cos^2\theta\sin^2\phi + \cos^2\phi}$$

$$= \frac{1}{1 + \cos^2\theta\tan^2\phi}$$

So

$$r'(\theta) = \frac{r\{\tan^{-1}(\tan\cos\phi)\}}{\sqrt{1 + \cos^2\theta\tan^2\phi}}$$

Let $r(\theta) = a_0 + a_2P_2(\cos\theta) + a_4P_4(\cos\theta) + a_6P_6(\cos\theta)$

$$r(\theta) = \sum_{k=0,2,4,6} a_kP_k(\cos\theta) \quad \text{where}$$

and let $r'(\theta) = \sum_{k=0,2,4,6} a_k'P_k(\cos\theta)$

$$\sum_{k=0,2,4,6} a_n' P_n(\cos\theta) = \sum_{k=0,2,4,6} a_k \frac{P_k\{\cos\{\tan^{-1}(\tan\theta\cos\phi)\}\}}{(1+\cos^2\theta\tan^2\phi)^{1/2}}$$

Multiply both sides by $P_j(\cos\theta)\sin\theta d\theta$ and integrate from $0 \to \pi$ using the property

$$\int_0^\pi P_k(\cos\theta)P_j(\cos\theta)\sin\theta d\theta = \frac{2}{2j+1}\delta_{kj}$$

$$\sum_{k=0,2,4,6} a_k' \int P_k(\cos\theta)P_j(\cos\theta)\sin\theta d\theta = \sum_{k=0,2,4,6} a_k \int_0^\pi \frac{P_k \cos\{\tan^{-1}(\tan\theta\cos\phi)\}}{(1+\cos^2\theta\tan^2\phi)^{1/2}}$$

$$\times P_j(\cos\theta)\sin\theta d\theta$$

Also notice that

$$\cos\alpha = \frac{1}{\sqrt{1+\tan^2\alpha}}$$

So

$$\cos\{\tan^{-1}(\tan\theta\cos\phi)\} = \frac{1}{(1+\tan^2\{\tan^{-1}(\tan\theta\cos\phi)\})^{1/2}}$$

$$= \frac{1}{(1+\tan^2\theta\cos^2\phi)^{1/2}}$$

And

$$a_j' = \frac{2j+1}{2} \sum_{k=0,2,4,6} a_n \int_0^\pi P_k \frac{\frac{1}{1+\tan^2\theta\cos^2\phi)^{1/2}}}{(1+\cos^2\theta\tan^2\phi)^{1/2}}$$

$$\times P_j(\cos\theta)\sin\theta d\theta$$

We must evaluate

$$\int_0^{\pi} \frac{P_n\left[\dfrac{1}{(1+\tan^2\theta\cos^2\phi)^{1/2}}\right]P_j(\cos\theta)\sin\theta d\phi}{(1+\cos^2\theta\tan^2\phi)^{1/2}}$$

Let $\cos\theta = x$

$$\tan^2\theta = \frac{1-\cos^2\theta}{\cos^2\theta} = \frac{1-x^2}{x^2}$$

$$\sin\theta d\theta = -dx$$

The integral becomes

$$\int_{-1}^{1} \frac{P_n\left[\dfrac{1}{(1+\frac{1-x^2}{x^2}\cos^2\phi)^{1/2}}\right]P_j(x)dx}{(1+x^2\tan^2\phi)^{1/2}}$$

For ϕ small

$$\cos^2\phi \approx 1-\phi^2$$

$$\tan^2\phi \approx \phi^2$$

Then:

$$\frac{1}{(1+x^2\phi^2)^{1/2}} \approx 1 - \frac{1}{2}\phi^2x^2$$

$$\left(1+\frac{1-x^2}{x^2}\cos^2\phi\right)^{-1/2} = \left(\frac{x^2+(1-x^2)(1-\phi^2)}{x^2}\right)^{-1/2}$$

$$= \frac{x}{\left[(x^2+(1-x^2)(1-\phi^2)\right]^{1/2}}$$

$$= \frac{x}{\{x^2+1-x^2-\phi^2(1-x^2)\}^{1/2}}$$

$$= x\{1+\frac{\phi^2}{2}(1-x^2)\}$$

$$= x + \frac{\phi^2}{2} x(1-x^2)$$

Then

$$P_k\{x + \frac{\phi^2}{2} x(1-x^2)\} \approx P_k(x) + \frac{dP_k(x)}{dx}\left(\frac{\phi^2}{2} x(1-x^2)\right) + \ldots$$

Putting this back into the integral we have:

$$\int_{-1}^{1} \{P_k(x) + \frac{dP_k}{dx} \quad \frac{\phi^2}{2} x(1-x^2)\} \quad P_j(x) \ \{1 - \frac{\phi^2}{2} x^2\} dx$$

$$= \int_{-1}^{1} \left\{P_k(x) + \frac{dP_k}{dx} \frac{\phi^2}{2} x(1-x^2) - P_k \frac{\phi^2}{2} x^2\right\} P_j(x) dx$$

$$= \int_{-1}^{1} P_k(x) P_j(x) dx + \frac{\phi^2}{2} \int_{-1}^{1} \left(\frac{dP_k(x)}{dx} x(1-x^2) - P_k(x) x^2\right) P_j(x) dx$$

$$= \frac{2}{2_{j+1}} \delta_{kj} + \frac{\phi^2}{2} \int_{-1}^{1} \left\{\frac{dP_k(x)}{dx} \ x\ (1-x^2) - P_k(x) x^2\right\} P_j(x) dx$$

Then

$$a_j' = a_j + \frac{2j+1}{2} \left(\frac{\phi^2}{2}\right) \sum_{k=0,2,4,6} a_k \int_{-1}^{1} \left\{\frac{dP_k(x)}{dx} x(1-x^2) - P_k(x) x^2\right\} P_j(x) dx$$

Let us call

$$A_{kj} = \int_{-1}^{1} \left\{\frac{dP_k(x)}{dx} x(1-x^2) - P_k(x) x^2\right\} P_j(x) dx$$

So

$$a_j' = a_j + \frac{2j+1}{2}\left(\frac{\phi^2}{2}\right) \sum_{k=0,2,4,6} a_k A_{kj}$$

We now must evaluate A_{kj}

Use the relation

$$(1-x^2)\,\frac{dP_k(x)}{dx} = kP_{k-1}(x) - kxP_k(x)$$

$$A_{kj} = \int_{-1}^{1}\left\{kxP_{k-1}(x) - kx^2P_k(x) - P_k(x)x^2\right\}P_j(x)dx$$

$$A_{kj} = \int_{-1}^{1} kxP_{k-1}(x)P_j(x)dx - (k+1)\int_{-1}^{1} x^2P_k(x)P_j(x)dx$$

Also since K,j = 0,2,4,6 P_k is even and P_{k-1} is odd:

$$A_{kj} = 2\left\{k\int_0^1 xP_{k-1}(x)P_j(x)dx - (k+1)\int_0^1 x^2P_k(x)P_j(x)dx\right\}$$

$A_{00} = -2/3$	$A_{02} = -4/15$	$A_{04} = 0$	$A_{06} = 0$
$A_{20} = 8/15$	$A_{22} = -2/21$	A_{24} $-24/105$	$A_{26} = 0$
$A_{40} = 0$	$A_{22} = 32/105$	$A_{24} = -38/693$	$A_{26} = -100/429$
$A_{60} = 0$	$A_{62} = 0$	$A_{64} = 40/143$	$A_{66} = -82/2145$

APPENDIX A3

Program which, given the normalized data, computes the coefficients of the first four even Legendre polynomials in a least squares fit.

TRIDENT

```
100 FILE #3:"COEFG"
101 FILE#4:"CHIG"
110 LET B=4
120 DIM S(4,4),M(4,4),A(4,1),C(4,1),P(4)
130 PRINT"INPUT THE DATA FILE AND AN EMPTY FILE"
140 INPUT A$,B$
150 FILE#1:A$
160 FILE#2:B$
170 SCRATCH#2
180 INPUT#1:X,Y
190 PRINT#2:X;",";Y
200 LET L=L+1
210 LET R=SQR(X*X+Y*Y)
220 LET Q=3.14159/2
230 IF Y=0 THEN 250
240 LET Q=ATN(X/Y)
250 LET P(1)=1
260 LET P(2)=(3*COS(2*Q)+1)/4
270 LET P(3)=(35*COS(4*Q)+20*COS(2*Q)+9)/64
280 LET P(4)=(231*COS(6*Q)+126*COS(4*Q)+105*COS(2*Q)+50)/512
290 FOR N=1 TO B
300 FOR M=1 TO B
310 LET S(N,M)=P(N)*P(M)+S(N,M)
320 NEXT M
330 NEXT N
340 FOR F=1 TO B
350 LET C(F,1)=R*P(F)+C(F,1)
360 NEXT F
370 IF MORE#1 THEN 180
380 MAT M=INV(S)
390 MAT A=M*C
400 MAT PRINT A
410 PRINT#3:A(1,1);",";A(2,1);",";A(3,1);",";A(4,1)
420 PRINT#2:1E37;",";1E37
430 FOR Q=0 TO 3.14159/2 STEP 3.14159/100
440 LET P0=1
450 LET P2=(3*COS(2*Q)+1)/4
460 LET P4=(35*COS(4*Q)+20*COS(2*Q)+9)/64
470 LET P6=(231*COS(6*Q)+126*COS(4*Q)+105*COS(2*Q)+50)/512
480 LET R=A(1,1)*P0+A(2,1)*P2+A(3,1)*P4+A(4,1)*P6
490 IF H=5 THEN 620
500 LET X=R*SIN(Q)
510 LET Y=R*COS(Q)
520 PRINT#2:X;",";Y
530 NEXT Q
540 LET H=5
550 RESET#1
560 INPUT#1:X,Y
570 LET R1=SQR(X*X+Y*Y)
580 LET Q=3.14159/2
```

TRIDENT (continued)

```
590 IF Y=0 THEN 610
600 LET Q=ATN(X/Y)
610 GO TO 440
620 LET K=K+(R1-R)^2/R1
630 IF MORE#1 THEN 560
640 LET K=K/L
650 PRINT"X^2 =";K
655 PRINT#4:K
660 END
```

APPENDIX A4

Program which utilizes a cubic spline fit and computes additional points in between given points.

SPLINFIT

```
100 LIBRARY "L.IG***:TELSUB","L.IG***:TYPSUB","L.IG***:CRTSUB"
110 LIBRARY "L.IG***:COMSUB"
120 '  THIS IS THE INPUT PORTION OF THE PROGRAM
130 PRINT
140 PRINT
150 DIM P(4,101),U(4,101),N(101,4),B(4,101),L(101),D(101)
160 PRINT "IS THE DATA IN AN INPUT FILE IN STANDARD GRAPHICAL FORMAT";
170 INPUT X$
180 IF X$="NO" THEN 220
190 PRINT "INPUT FILE NAME";
200 INPUT B$
210 FILE #2:B$
220 PRINT "ENTER NAME OF OUTPUT FILE";
230 INPUT D$
240 FILE #1:D$
250 SCRATCH #1
260 PRINT "SPACE OR PLANE CURVE";
270 INPUT B$
280 IF X$="NO" THEN 560
290 IF SEG$(B$,1,3)="PLA" THEN 500
300 IF SEG$(B$,1,3)="SPA" THEN 330
310 PRINT "ILLEGAL OPTION, RETYPE";
320 GO TO 270
330 FOR I=1 TO 4
340 FOR J=1 TO 101
350 LET P(I,J)=0
360 LET U(I,J)=0
370 LET N(J,I)=0
380 LET B(I,J)=0
390 LET L(J)=0
400 LET D(J)=0
410 NEXT J
420 NEXT I
430 LET J=0
440 IF SEG$(B$,1,3)="PLA" THEN 500
450 LET J=J+1
460 IF END#2 THEN 550
470 INPUT #2:P(1,J),P(2,J),P(3,J)
480 IF P(1,J)=1E37 THEN 550
490 GO TO 450
500 LET J=J+1
510 IF END #2 THEN 550
520 INPUT #2:P(1,J),P(2,J)
530 IF P(1,J)=1E37 THEN 550
540 GO TO 500
550 IF J=1 THEN 980
560 IF SEG$(B$,1,3)="SPA" THEN 620
570 IF SEG$(B$,1,3)="PLA" THEN 600
580 PRINT "ILLEGAL OPTION, RETYPE";
590 GO TO 270
```

SPLINFIT (continued)

```
600 LET S=2
610 GO TO 630
620 LET S=3
630 LET N=J-1
640 IF X$="NO" THEN 660
650 GO TO 760
660 PRINT "INPUT NUMBER OF POINTS TO BE ENTERED";
670 INPUT N
680 PRINT "INPUT POINT X,Y, AND (IF NECESSARY), Z COMPONENTS"
690 PRINT "ONE SET AT A TIME"
700 FOR J=1 TO N
710 IF S=3 THEN 740
720 INPUT P(1,J),P(2,J)
730 GO TO 750
740 INPUT P(1,J),P(2,J),P(3,J)
750 NEXT J
760 LET R=R+1
770 PRINT
780 PRINT
790 PRINT "CURVE";R;":"
800 LET Z9=0
810 PRINT
820 PRINT"INPUT INITIAL END CONDITION";
830 INPUT A$
840 PRINT
850 IF SEG$(A$,1,3)= "CYC" THEN 930
860 IF SEG$(A$,1,3)= "ANT" THEN 930
870 CALL "ENDPNT":S,N,P( , ),N( , ),B( , ),D( ),L( ),Z,U( , ),A$,F$,Z9
880 IF Z9=1 THEN 800
890 IF SEG$(A$,1,1)= "Q" THEN 930
900 IF SEG$(F$,1,1)= "Q" THEN 930
910 CALL "MATOPS":S,N,P( , ),N( , ),B( , ),D( ),L( ),U( , )
920 GO TO 940
930 CALL "MATINV":S,N,P( , ),N( , ),B( , ),D( ),L( ),U( , ),A$,F$,Z
940 CALL "CURGEN":S,N,P( , ),L( ),Z,U( , ),#1
950 LET W=Z*(N-1)+2
960 IF X$="NO" THEN 980
970 GO TO 330
980 CALL "GRAPH":W,#1,S,D$
990 PRINT "DO YOU WANT ANOTHER PLOT OF THE SAME CURVE";
1000 INPUT A$
1010 IF A$="NO" THEN 1060
1020 RESET #2
1030 SCRATCH #1
1040 LET R=0
1050 GO TO 330
1060 END
1070 REM SETS UP MATRIX END PTS FOR REL,CLA,P,Q CONDITIONS
1080 SUB "ENDPNT":S,N,P( , ),N( , ),B( , ),D( ),L( ),Z,U( , ),A$,B$,Z9
1090 IF SEG$(A$,1,1) = "P" THEN 1300
```

SPLINFIT (continued)

```
1100 IF SEG$(A$,1,1) = "Q" THEN 1320
1110 IF SEG$(A$,1,3) = "REL" THEN 1270
1120 IF SEG$(A$,1,3)= "CLA" THEN 1160
1130 PRINT"ILLEGAL INITIAL CONDITION";A$;"RETYPE"
1140 LET Z9=1
1150 GO TO 2040
1160 PRINT "INPUT INITIAL END TANGENT VECTOR COMPONENTS";
1170 IF S=3 THEN 1200
1180 INPUT U(1,1),U(2,1)
1190 GO TO 1210
1200 INPUT U(1,1),U(2,1),U(3,1)
1210 LET N(1,2)=1
1220 LET N(1,3)=0
1230 FOR K=1 TO S
1240 LET B(K,1)=U(K,1)
1250 NEXT K
1260 GO TO 1320
1270 LET N(1,2)=1
1280 LET N(1,3)=.5
1290 GO TO 1320
1300 LET N(1,2)=1
1310 LET N(1,3)=1
1320 FOR J=1 TO N-1
1330 IF S=3 THEN 1370
1340 LET D(J)=SQR((P(1,J+1)-P(1,J))^2+(P(2,J+1)-P(2,J))^2)
1350 LET L(J)=D(J)
1360 GO TO 1390
1370 LET D(J)=SQR((P(1,J+1)-P(1,J))^2+(P(2,J+1)-P(2,J))^2+(P(3,J+1)-P(3,J))^2)
1380 LET L(J)=D(J)
1390 NEXT J
1400 IF SEG$(A$,1,3)= "CLA" THEN 1600
1410 IF SEG$(A$,1,1)= "P" THEN 1480
1420 IF SEG$(A$,1,1)= "Q" THEN 1520
1430 CHANGE A TO A$
1440 FOR K=1 TO S
1450 LET B(K,1)=(3/(2*L(1)))*(P(K,2)-P(K,1))
1460 NEXT K
1470 GO TO 1600
1480 FOR K=1 TO S
1490 LET B(K,1)=(2/L(1))*(P(K,2)-P(K,1))
1500 NEXT K
1510 GO TO 1600
1520 REM  TREAT Q-SPLINE CONDITIONS
1530 LET S1=L(1)/L(2)
1540 LET N(1,1)=1
1550 LET N(1,2)=1-S1^2
1560 LET N(1,3)=-S1^2
1570 FOR K=1 TO S
1580 LET B(K,1)=(2/L(1))*(-P(K,1)+(1+S1^3)*P(K,2)-(S1^3)*P(K,3))
1590 NEXT K
```

SPLINFIT (continued)

```
1600 PRINT
1610 PRINT"INPUT FINAL END CONDITION";
1620 INPUT B$
1630 IF SEG$(B$,1,1)="P" THEN 1870
1640 IF SEG$(B$,1,1)="Q" THEN 1930
1650 IF SEG$(B$,1,3)="REL" THEN 1810
1660 IF SEG$(B$,1,3)="CLA" THEN 1700
1670 PRINT "ILLEGAL OPTION, RETYPE";
1680 GO TO 1610
1690 ' TEST POINT
1700 PRINT "INPUT FINAL END TANGENT VECTOR COMPONENTS";
1710 IF S=3 THEN 1740
1720 INPUT U(1,N),U(2,N)
1730 GO TO 1750
1740 INPUT U(1,N),U(2,N),U(3,N)
1750 LET N(N,1)=0
1760 LET N(N,2)=1
1770 FOR K=1 TO S
1780 LET B(K,N)=U(K,N)
1790 NEXT K
1800 GO TO 2000
1810 LET N(N,1)=2
1820 LET N(N,2)=4
1830 FOR K=1 TO S
1840 LET B(K,N)=(6/L(N-1))*(P(K,N)-P(K,N-1))
1850 NEXT K
1860 GO TO 2000
1870 LET N(N,1)=1
1880 LET N(N,2)=1
1890 FOR K=1 TO S
1900 LET B(K,N)=(2/L(N-1))*(P(K,N)-P(K,N-1))
1910 NEXT K
1920 GO TO 2000
1930 LET S2=L(N-1)/L(N-2)
1940 LET N(N,1)=-S2^2
1950 LET N(N,2)=1-S2^2
1960 LET N(N,3)=1
1970 FOR K=1 TO S
1980 LET B(K,N)=(2/L(N-1))*((S2^3)*P(K,N-2)-(1+S2^3)*P(K,N-1)+P(K,N))
1990 NEXT K
2000 PRINT
2010 PRINT"NUMBER OF INTERMEDIATE POINTS PER SPAN";
2020 INPUT Z
2030 LET Z=Z+1
2040 SUBEND
2050' THE FOLLOWING SETS UP THE INTERIOR PORTION OF THE MATRIX
2060' NOTE- HERE I USE A DIAGONAL MATRIX TO SAVE STORAGE SPACE, AND
2070' EMPLOY APPROPRIATE ALGORITHMS INSTEAD OF MAT FUNCTIONS.
2080 SUB "MATOPS":S,N,P( , ),N( , ),B( , ),D( ),L( ),U( , )
2090 FOR J=2 TO N-1
```

SPLINFIT (continued)

```
2100 LET N(J,1)=L(J)
2110 LET N(J,2)=2*(L(J)+L(J-1))
2120 LET N(J,3)=L(J-1)
2130 FOR K=1 TO S
2140 LET B(K,J)=3*(L(J-1)^2*(P(K,J+1)-P(K,J))+L(J)^2*(P(K,J)-P(K,J-1)))
2150 LET B(K,J)=B(K,J)/(L(J)*L(J-1))
2160 NEXT K
2170 NEXT J
2180' THE FOLLOWING IS THE GAUSSIAN ELIMINATION ON THE MATRIX,
2190 FOR I=2 TO N
2200 IF N(I,1)=0 THEN 2310
2210 LET D=N(I-1,2)/N(I,1)
2220 FOR K=1 TO 3
2230 LET N(I,K)=N(I,K)*D-N(I-1,K+1)
2240 LET B(K,I)=B(K,I)*D-B(K,I-1)
2250 NEXT K
2260 LET Q=N(I,2)
2270 FOR K=1 TO 3
2280 LET N(I,K)=N(I,K)/Q
2290 LET B(K,I)=B(K,I)/Q
2300 NEXT K
2310 NEXT I
2320 FOR K=1 TO S
2330 FOR J=0 TO N-1
2340 LET U(K,N-J)=(B(K,N-J)-N(N-J,3)*U(K,N+1-J))/N(N-J,2)
2350 NEXT J
2360 NEXT K
2370 SUBEND
2380' THE BASIC TANGENT VECTORS ARE NOW AVAILABLE HERE.
2390' THE FOLLOWING MODIFIES THE VECTOR MAGNITUDES TO EQUAL THE
2400' SHORTER OF THE CHORD LENGTHS TO ADJACENT POINTS FOR EACH POINT.
2410 SUB "TANMOD":S,N,U( , ),D( )
2420 FOR J=2 TO N-1
2430 IF S=3 THEN 2460
2440 LET U=SQR(U(1,J)^2+U(2,J)^2)
2450 GO TO 2470
2460 LET U=SQR(U(1,J)^2+U(2,J)^2+U(3,J)^2)
2470 IF D(J-1)<D(J) THEN 2520
2480 FOR K=1 TO S
2490 LET U(K,J)=(U(K,J)*D(J))/U
2500 NEXT K
2510 GO TO 2550
2520 FOR K=1 TO S
2530 LET U(K,J)=(U(K,J)*D(J-1))/U
2540 NEXT K
2550 NEXT J
2560 LET J=1
2570 IF S=3 THEN 2600
2580 LET U=SQR(U(1,J)^2+U(2,J)^2)
2590 GO TO 2610
```

SPLINFIT (continued)

```
2600 LET U=SQR(U(1,J)^2+U(2,J)^2+U(3,J)^2)
2610 IF J=N THEN 2640
2620 LET F=D(J)
2630 GO TO 2650
2640 LET F=D(J-1)
2650 FOR K=1 TO S
2660 LET U(K,J)=(U(K,J)*F)/U
2670 NEXT K
2680 IF J=N THEN 2710
2690 LET J=N
2700 GO TO 2570
2710 SUBEND
2720' THE FOLLOWING SOLVES FOR THE PARAMETRIC COEFFICIENTS AND
2730' FILLS IN INTERMEDIATE POINTS BETWEEN THE SPECIFIED POINTS,
2740' STORING THE DATA IN AN OUTPUT FILE IN STANDARD GRAPHICAL
2750' FORMAT
2760 SUB "CURGEN":S,N,P( , ),L( ),Z,U( , ),#1
2770 PRINT "DO YOU WANT A LIST OF POINT RESULTS";
2780 INPUT F$
2790 IF F$="NO" THEN 2830
2800 PRINT
2810 PRINT "POINT";TAB(7);"F'(X)";TAB(20);"F'(Y)";TAB(27);"F'(Z)";
2820 PRINT TAB(37);"F''(X)";TAB(50);"F''(Y)";TAB(62);"F''(Z)"
2830 FOR J=1 TO N-1
2840 FOR K=1 TO S
2850 LET F(1,K)=P(K,J)
2860 LET F(2,K)=U(K,J)
2870 LET F(3,K)=(3/L(J)^2)*(P(K,J+1)-P(K,J))-(1/L(J))*(U(K,J+1)+2*U(K,J))
2880 LET F(4,K)=(-2/L(J)^3)*(P(K,J+1)-P(K,J))+(1/L(J)^2)*(U(K,J+1)+U(K,J))
2890 NEXT K
2900 IF F$="NO" THEN 2970
2910 IF S=3 THEN 2950
2920 PRINT J;TAB(7);F(2,1);TAB(20);F(2,2);TAB(27);0;TAB(37);
2930 PRINT 2*F(3,1);TAB(50);2*F(3,2);TAB(62);0
2940 GO TO 2970
2950 PRINT J;TAB(7);F(2,1);TAB(20);F(2,2);TAB(27);F(2,3);TAB(37);
2960 PRINT 2*F(3,1);TAB(50);2*F(3,2);TAB(62);2*F(3,3)
2970 FOR T=0 TO L(J) STEP L(J)/Z
2980 IF J=1 THEN 3010
2990 IF T<>0 THEN 3010
3000 GO TO 3080
3010 FOR K=1 TO S
3020 LET C(K)=F(1,K)+F(2,K)*T+F(3,K)*(T^2)+F(4,K)*(T^3)
3030 NEXT K
3040 IF S=3 THEN 3070
3050 PRINT #1:C(1);",";C(2)
3060 GO TO 3080
3070 PRINT #1:C(1);",";C(2);",";C(3)
3080 NEXT T
3090 NEXT J
[illegible]
```

SPLINFIT (continued)

```
3100 IF F$="NO" THEN  3220
3110 PRINT J+1;TAB(7);F(2,1)+2*F(3,1)*L(J)+3*F(4,1)*L(J)^2;TAB(20);
3120 PRINT F(2,2)+2*F(3,2)*L(J)+3*F(4,2)*L(J)^2;TAB(27);
3130 IF S=3 THEN 3160
3140 PRINT 0;TAB(37);
3150 GO TO 3170
3160 PRINT F(2,3)+2*F(3,3)*L(J)+3*F(4,3)*L(J)^2;TAB(37);
3170 PRINT 2*F(3,1)+6*F(4,1)*L(J);TAB(50);2*F(3,2)+6*F(4,1)*L(J);TAB(62);
3180 IF S=3 THEN 3210
3190 PRINT 0
3200 GO TO 3220
3210 PRINT 2*F(3,3)+6*F(4,3)*L(J)
3220 IF S=3 THEN 3250
3230 PRINT #1:"1E37,1E37"
3240 GO TO 3260
3250 PRINT #1:"1E37,1E37,1E37"
3260 SUBEND
3270 SUB "GRAPH":N,#1,S,D$
3280 RESET #1
3290 IF S=2 THEN 3310
3300 CALL "TRANS":#1
3310 DIM X(500),Y(500)
3320 LET I=0
3330 LET I=I+1
3340 IF END#1 THEN 3370
3350 INPUT #1:X(I),Y(I)
3360 GO TO 3330
3370 LET N=I-1
3380 PRINT "IS THE OUTPUT TO BE DISPLAYED ON TELETYPE,CRT,"
3390 PRINT "TYPAGRAPH,COMPUTEK,OR LATER";
3400 INPUT Z$
3410 IF Z$="TELETYPE" THEN 3480
3420 IF Z$="CRT" THEN 3500
3430 IF Z$="TYPAGRAPH" THEN 3520
3440 IF Z$="COMPUTEK" THEN 3540
3450 IF Z$="LATER" THEN 3560
3460 PRINT "INCORRECT FORMAT, TRY AGAIN"
3470 GO TO 3380
3480 CALL "TELSUB":#1,0,A$,3
3490 GO TO 3570
3500 CALL "CRTSUB":#1,0,A$,3
3510 GO TO 3570
3520 CALL "TYPSUB":#1,0,A$,3
3530 GO TO 3570
3540 CALL "COMSUB":#1,0,A$,3
3550 GO TO 3570
3560 PRINT "POINTS ARE LOCATED AS SPECIFIED IN FILE ";D$
3570 SUBEND
3580 SUB "TRANS":#1
3590 PRINT "INPUT NAME OF SCRATCH FILE";
```

SPLINFIT (continued)

```
3600 INPUT B$
3610 FILE #2:B$
3620 SCRATCH #2
3630 PRINT "TYPE OF PROJECTION:(1=X-Y,2=Y-Z,3=Z-X)"
3640 INPUT A
3650 ON A GO TO 3660,3710,3760
3660 IF MORE #1 THEN 3680
3670 GO TO 3810
3680 INPUT #1:A,B,C
3690 PRINT #2:A;",";B
3700 GO TO 3660
3710 IF MORE #1 THEN 3730
3720 GO TO 3810
3730 INPUT #1:A,B,C
3740 PRINT #2:B;",";C
3750 GO TO 3710
3760 IF MORE #1 THEN 3780
3770 GO TO 3810
3780 INPUT #1:A,B,C
3790 PRINT #2:C;",";A
3800 GO TO 3760
3810 SCRATCH #1
3820 RESET #2
3830 INPUT #2:A,B
3840 PRINT #1:A;",";B
3850 IF END #2 THEN 3870
3860 GO TO 3830
3870 RESET #1
3880 SUBEND
3890 SUB "MATINV":S,N,P( , ),N( , ),B( , ),D( ),L( ),U( , ),A$,B$,Z
3900 DIM M(70,70),C(70),V(70,70),W(70)
3910 IF SEG$(A$,1,3)="CYC" THEN 3980
3920 IF SEG$(A$,1,3)="ANT" THEN 3980
3930 MAT M=ZER(N,N)
3940 MAT C=ZER(N)
3950 MAT W=ZER(N)
3960 MAT V=ZER(N,N)
3970 GO TO 4020
3980 MAT M=ZER(N-1,N-1)
3990 MAT C=ZER(N-1)
4000 MAT W=ZER(N-1)
4010 MAT V=ZER(N-1,N-1)
4020 IF SEG$(A$,1,3)="CYC" THEN 4190
4030 IF SEG$(A$,1,3)="ANT" THEN 4190
4040 IF SEG$(A$,1,1)="Q" THEN 4080
4050 LET M(1,1)=N(1,2)
4060 LET M(1,2)=N(1,3)
4070 GO TO 4110
4080 LET M(1,1)=N(1,1)
4090 LET M(1,2)=N(1,2)
```

SPLINFIT (continued)

```
4100 LET M(1,3)=N(1,3)
4110 IF SEG$(B$,1,1)="O" THEN 4150
4120 LET M(N,N-1)=N(N,1)
4130 LET M(N,N)=N(N,2)
4140 GO TO 4450
4150 LET M(N,N-2)=N(N,1)
4160 LET M(N,N-1)=N(N,2)
4170 LET M(N,N)=N(N,3)
4180 GO TO 4450
4190 FOR J=1 TO N-1
4200 IF S=3 THEN 4240
4210 LET D(J)=SQR((P(1,J+1)-P(1,J))^2+(P(2,J+1)-P(2,J))^2)
4220 LET L(J)=D(J)
4230 GO TO 4260
4240 LET D(J)=SQR((P(1,J+1)-P(1,J))^2+(P(2,J+1)-P(2,J))^2+(P(3,J+1)-P(3,J))^2)
4250 LET L(J)=D(J)
4260 NEXT J
4270 LET S3=L(N-1)/L(1)
4280 IF SEG$(A$,1,3)="ANT" THEN 4360
4290 LET M(1,1)=2+2*S3
4300 LET M(1,2)=S3
4310 LET M(1,N-1)=1
4320 FOR K=1 TO S
4330 LET B(K,1)=(3/L(1))*(S3*(P(K,2)-P(K,1))+(1/S3)*(P(K,N)-P(K,N-1)))
4340 NEXT K
4350 GO TO 4420
4360 LET M(1,1)=2+2*S3
4370 LET M(1,2)=S3
4380 LET M(1,N-1)=-1
4390 FOR K=1 TO S
4400 LET B(K,1)=(3/L(1))*(S3*(P(K,2)-P(K,1))-(1/S3)*(P(K,N)-P(K,N-1)))
4410 NEXT K
4420 PRINT"NUMBER OF INTERMEDIATE POINTS PER SPAN";
4430 INPUT Z
4440 LET Z=Z+1
4450 REM SET UP INTERIOR MATRIX AND INVERT
4460 FOR J=2 TO N-1
4470 LET M(J,J-1)=L(J)
4480 LET M(J,J)=2*(L(J)+L(J-1))
4490 IF J<>N-1 THEN 4540
4500 IF SEG$(A$,1,3)="CYC" THEN 4530
4510 IF SEG$(A$,1,3)="ANT" THEN 4530
4520 GO TO 4540
4530 GO TO 4550
4540 LET M(J,J+1)=L(J-1)
4550 FOR K=1 TO S
4560 LET B(K,J)=3*(L(J-1)^2*(P(K,J+1)-P(K,J))+L(J)^2*(P(K,J)-P(K,J-1)))
4570 LET B(K,J)=B(K,J)/(L(J)*L(J-1))
4580 NEXT K
4590 NEXT J
4600 M
```

SPLINFIT (continued)

```
4600 MAT V=INV(M)
4610 IF SEG$(A$,1,3)="CYC" THEN 4730
4620 IF SEG$(A$,1,3)="ANT" THEN 4730
4630 FOR K=1 TO S
4640 FOR J=1 TO N
4650 LET C(J)=B(K,J)
4660 NEXT J
4670 MAT W=V*C
4680 FOR J=1 TO N
4690 LET U(K,J)=W(J)
4700 NEXT J
4710 NEXT K
4720 GO TO 4900
4730 FOR K=1 TO S
4740 FOR J=1 TO N-1
4750 LET C(J)=B(K,J)
4760 NEXT J
4770 MAT W=V*C
4780 FOR J=1 TO N-1
4790 LET U(K,J)=W(J)
4800 NEXT J
4810 NEXT K
4820 IF SEG$(A$,1,3)="ANT" THEN 4870
4830 FOR K=1 TO S
4840 LET U(K,N)=U(K,1)
4850 NEXT K
4860 GO TO 4900
4870 FOR K=1 TO S
4880 LET U(K,N)=-U(K,1)
4890 NEXT K
4900 SUBEND
```

APPENDIX A5

Coefficients computed by "Trident" program for both cases.

COEFFICIENTS FOR EXPANSION OF BUBBLE-CASE 1

A0	A2	A4	A6
0.695397	0.412924	-0.140418	5.00495 E-2
0.632829	0.355654	-0.121983	5.96184 E-2
0.567656	0.400168	-0.123263	3.51356 E-2
0.563461	0.321668	-9.88701 E-2	4.54331 E-2
0.5126	0.242358	-5.75205 E-2	3.68124 E-2
0.487923	0.225188	-9.37463 E-2	5.5635 E-3
0.509801	0.230113	-0.15733	3.15432 E-2
0.536802	9.79686 E-2	-0.179822	-1.19548 E-2
0.507123	-5.00193 E-2	-0.221311	1.97178 E-2
0.500335	-8.56244 E-2	-0.258396	1.43054 E-3

*

COEFFICIENTS FOR EXPANSION OF BUBBLE-CASE 2

A0	A2	A4	A6
0.681519	0.444012	-0.210683	9.44173 E-2
0.685496	0.412312	-0.210071	0.096682
0.68136	0.354767	-0.143659	7.10024 E-2
0.66308	0.359718	-0.139868	6.56617 E-2
0.638041	0.364293	-0.111248	5.17293 E-2
0.590996	0.426635	-0.108948	3.94992 E-2
0.545938	0.38489	-0.091815	5.19594 E-2
0.520715	0.313837	-1.99842 E-2	2.28483 E-2
0.464311	0.27543	1.74285 E-2	2.29671 E-2
0.427852	0.219103	3.42362 E-2	5.23286 E-2
0.370364	0.186245	1.53092 E-3	0.092001
0.342797	0.116947	-3.43396 E-2	6.32129 E-2
0.33547	0.040418	-0.113346	-3.14466 E-2
0.359263	-5.14157 E-3	-0.139174	-8.07007 E-2

*

APPENDIX A6

Values for X^2 Goodness-of-fit Test for both cases.

CASE 1

FRAME	X^2
1	1.13169 E-3
2	1.66658 E-3
3	1.14931 E-4
4	3.34727 E-4
5	4.78711 E-4
6	9.4867 E-5
7	5.74483 E-5
8	5.69113 E-4
9	1.96173 E-3
10	1.45965 E-3

*

*

CASE 2

FRAME	X^2
1	1.51453 E-2
2	0.02603
3	2.23721 E-2
4	1.30353 E-2
5	8.17185 E-3
6	6.82436 E-3
7	3.09257 E-2
8	1.53104 E-2
9	6.51845 E-3
10	4.46423 E-3
11	7.06414 E-3
12	6.78229 E-3
13	0.100918
14	0.16202

APPENDIX A7

Program written for the USNA PDP-11, which generates a three dimensional display for the E+S Picture System.

AKPLOT

```
100 OPEN "AKCOEF.DAT" FOR INPUT AS FILE #3
110 INPUT #3:M
120 DIM C(72,4),D(599),A(4)
130 FOR I=1 TO M
140 INPUT #3:C(I,1),C(I,2),C(I,3),C(I,4)
150 NEXT I
160 CALL "PSNT"(2,0)
170 H=16300
180 LET V=30
190 V=15
200 V9=1.00000E-03
210 LET S9=.125663
220 S9=S9/2
230 P=2*H
240 LET S=10
250 CALL "WIND"(-H,H,-H,H,H,-H,P)
260 T=-1000
270 CALL "TRAN"(0,0,T)
280 B=0
290 PRINT B
300 CALL "ROT"(B,1)
310 FOR C=1 TO M
320 FOR I=1 TO 4
330 LET A(I)=C(C,I)
340 NEXT I
350 GOSUB 490
360 FOR A=0 TO 360 STEP S
370 CALL "PUSH"
380 CALL "ROT"(A,2)
390 CALL "DR3D"(D,INT(I/3),2,2)
400 CALL "POP"
410 NEXT A
420 CALL "NFRM"
430 CALL "SWCH"(0,Q9)
440 IF Q9<>1 THEN 470
450 CALL "RSTP"
460 STOP
470 NEXT C
480 STOP
490 REM
500 LET I=0
510 FOR Q=0 TO 1.5708 STEP S9
520 LET P0=1
530 LET P2=(3*COS(2*Q)+1)/4
540 LET P4=(35*COS(4*Q)+20*COS(2*Q)+9)/64
550 LET P6=(231*COS(6*Q)+126*COS(4*Q)+105*COS(2*Q)+50)/512
560 LET R=A(1)*P0+A(2)*P2+A(3)*P4+A(4)*P6
570 LET X=R*SIN(Q)
580 LET Y=R*COS(Q)
590 IF Y<0 THEN 670
```

AKPLOT (continued)

```
600 IF ABS(X)<V9 THEN 670
610 LET D(I)=INT(X*1000*V)
620 LET I=I+1
630 LET D(I)=INT(Y*1000*V)
640 LET I=I+1
650 LET D(I)=INT(0)
660 LET I=I+1
670 NEXT Q
680 RETURN
690 END
```

APPENDIX A8

Program for hard copy generation of three dimensional display from PDP-11/E+S Picture System on Xynetics plotter.

AD-A032 717 NAVAL ACADEMY ANNAPOLIS MD F/G 20/4
CYCLIC LIQUID JET BEHAVIOR IN PULSATING BUBBLES.(U)
MAY 76 N E KARANGELEN
UNCLASSIFIED USNA-TSPR-79 NL

2 OF 2
AD
A032717

END
DATE
FILMED
1 — 77

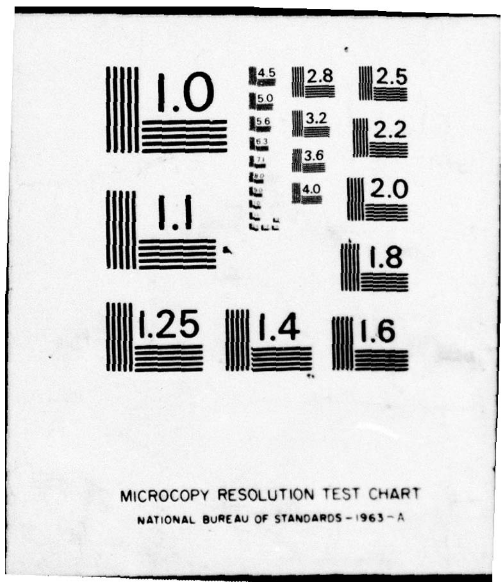
1.0
1.1
1.25
1.4
1.6
1.8
2.0
2.2
2.5
2.8
3.2
3.6
4.0
4.5
5.0
5.6
6.3
MICROCOPY RESOLUTION TEST CHART
NATIONAL BUREAU OF STANDARDS-1963-A

AKFTBD

```
100 OPEN "AKCOEF.DAT" FOR INPUT AS FILE #3
110 INPUT #3:M
120 DIM C(72,4),D(599),A(4)
130 REM
140 FOR I=1 TO M
150 INPUT #3:C(I,1),C(I,2),C(I,3),C(I,4)
160 NEXT I
170 CALL "PSNT"(2,0)
180 LET H=16000
190 LET V=1
200 LET V9=.2
210 LET S9=.125663
220 S9=S9/2
230 LET V8=0
240 P=2*H
250 LET S=10
260 LET B=50
270 FOR C=1 TO M
280 FOR I=1 TO 4
290 LET A(I)=C(C,I)
300 NEXT I
310 CALL "INST"(-2000,2000,22000-V8,26000-V8,2000,-2000)
320 LET V8=V8+5000
330 GOSUB 520
340 CALL "WIND"(-H,H,-H,H,H,-H)
350 CALL "MAST"(-H,H,-H,H,H,-H)
360 CALL "ROT"(B,1)
370 FOR A=0 TO 360 STEP S
380 CALL "PUSH"
390 CALL "ROT"(A,2)
400 CALL "DR3D"(D,INT(I/3),2,2)
410 CALL "POP"
420 NEXT A
430 CALL "POP"
440 NEXT C
450 CALL "NFRM"
460 CALL "LITE"(0,1)
470 CALL "SWCH"(0,Q9)
480 IF Q9<>1 THEN 470
490 CALL "LITE"(0,0)
500 CALL "RSTP"
510 STOP
520 REM
530 LET I=0
540 FOR Q=0 TO 1.5708 STEP S9
550 LET C2=COS(2*Q)
560 LET C4=COS(4*Q)
570 LET C6=COS(6*Q)
580 LET P0=1
590 LET P2=(3*C2+1)/4
```

AKFTBD (continued)

```
600 LET P4=(35*C4+20*C2+9)/64
610 LET P6=(231*C6+126*C4+105*C2+50)/512
620 LET R=A(1)*P0+A(2)*P2+A(3)*P4+A(4)*P6
630 LET X=R*COS(Q)
640 LET Y=R*SIN(Q)
650 LET Y=Y-.5
660 IF Y<0 THEN 740
670 IF ABS(X)<V9 THEN 740
680 LET D(I)=INT(X*1000*V)
690 LET I=I+1
700 LET D(I)=INT(Y*1000*V)
710 LET I=I+1
720 LET D(I)=INT(0)
730 LET I=I+1
740 NEXT Q
750 RETURN
760 END
```

UNCLASSIFIED
Security Classification

DOCUMENT CONTROL DATA - R & D

(Security classification of title, body of abstract and indexing annotation must be entered when the overall report is classified)

1. ORIGINATING ACTIVITY (Corporate author) U.S. Naval Academy, Annapolis.	2a. REPORT SECURITY CLASSIFICATION UNCLASSIFIED 2b. GROUP
3. REPORT TITLE Cyclic liquid jet behavior in pulsating bubbles.	
4. DESCRIPTIVE NOTES (Type of report and inclusive dates) Research report.	
5. AUTHOR(S) (First name, middle initial, last name) Nicholas E. Karangelen.	
6. REPORT DATE 17 May 1976.	7a. TOTAL NO. OF PAGES 96 — 7b. NO. OF REFS 20
8a. CONTRACT OR GRANT NO. b. PROJECT NO. c. d.	9a. ORIGINATOR'S REPORT NUMBER(S) U.S. Naval Academy, Annapolis - Trident Scholar project report, no. 79 (1976) 9b. OTHER REPORT NO(S) (Any other numbers that may be assigned this report)
10. DISTRIBUTION STATEMENT This document has been approved for public release ; its distribution is UNLIMITED.	
11. SUPPLEMENTARY NOTES	12. SPONSORING MILITARY ACTIVITY U.S. Naval Academy, Annapolis.

13. ABSTRACT

The report concerns the behavior of cyclic liquid jets in pulsating bubbles.

The jets were developed in bubbles which were situated on a vibrating platform that was contained within a vessel capable of sustaining reduced pressures. The entire assembly was mounted on a variable frequency vibration table and driven at displacement amplitudes on the order of a millimeter. The reduced pressure enabled the jets to be quite easily formed within the vessel ; the jets were formed in bubbles containing both vapor and gas, thus resulting in bubbles exhibiting jet behavior over several cycles. The bubbles were photographed with a high speed camera and a detailed analysis made of the behavior of the jet as a function of time.

It was found that the bubble surface could be well represented by the first four even terms of a Legendre polynomial expansion. Further, a graphic three-dimensional display of the bubble surface, generated by the expansion, gives excellent agreement with the observed behavior.

Data of calculations is given in the appendices.

UNCLASSIFIED.
Security Classification